

# CD95 co-stimulation blocks activation of naive T cells by inhibiting T cell receptor signaling

Gudrun Strauss,<sup>1</sup> Jonathan A. Lindquist,<sup>2</sup> Nathalie Arhel,<sup>3</sup> Edward Felder,<sup>4</sup> Sabine Karl,<sup>1</sup> Tobias L. Haas,<sup>5</sup> Simone Fulda,<sup>1</sup> Henning Walczak,<sup>6</sup> Frank Kirchhoff,<sup>3</sup> and Klaus-Michael Debatin<sup>1</sup>

<sup>1</sup>University Children's Hospital Ulm, 89075 Ulm, Germany

<sup>2</sup>Institute of Molecular and Clinical Immunology, Otto-von-Guericke University, 39120 Magdeburg, Germany

<sup>3</sup>Institute of Virology and <sup>4</sup>Institute of General Physiology, University of Ulm, 89075 Ulm, Germany

<sup>5</sup>Division of Apoptosis Regulation, German Cancer Research Center, 69120 Heidelberg, Germany

<sup>6</sup>Department of Immunology, Division of Medicine, Imperial College London, London W12 0NN, UK

CD95 is a multifunctional receptor that induces cell death or proliferation depending on the signal, cell type, and cellular context. Here, we describe a thus far unknown function of CD95 as a silencer of T cell activation. Naive human T cells triggered by antigen-presenting cells expressing a membrane-bound form of CD95 ligand (CD95L) or stimulated by anti-CD3 and -CD28 antibodies in the presence of recombinant CD95L had reduced activation and proliferation, whereas preactivated, CD95-sensitive T cells underwent apoptosis. Triggering of CD95 during T cell priming interfered with proximal T cell receptor signaling by inhibiting the recruitment of  $\zeta$ -chain-associated protein of 70 kD, phospholipase- $\gamma$ , and protein kinase C- $\theta$  into lipid rafts, thereby preventing their mutual tyrosine protein phosphorylation. Subsequently,  $\text{Ca}^{2+}$  mobilization and nuclear translocation of transcription factors NFAT, AP1, and NF- $\kappa$ B were strongly reduced, leading to impaired cytokine secretion. CD95-mediated inhibition of proliferation in naive T cells could not be reverted by the addition of exogenous interleukin-2 and T cells primed by CD95 co-stimulation remained partially unresponsive upon secondary T cell stimulation. HIV infection induced CD95L expression in primary human antigen-presenting cells, and thereby suppressed T cell activation, suggesting that CD95/CD95L-mediated silencing of T cell activation represents a novel mechanism of immune evasion.

## CORRESPONDENCE

Gudrun Strauss:  
gudrun.strauss@uniklinik-ulm.de

Abbreviations used: AAD, amino-actinomycin-D; CD95L, CD95 ligand; DEVD, Asp-Glu-Val-Asp; EMSA, electrophoretic mobility shift assay; IETD, Ile-Glu-Thr-Asp; LAT, linker of activated T cells; m-CD95L, membrane-bound CD95L; MAPK, mitogen-activated protein kinase; PKC, protein kinase C; PLC, phospholipase C; SEE, staphylococcal enterotoxin E; Z-VAD.fmk, Z-Val-Ala-DL-Asp-fluoromethylketone; ZAP70,  $\zeta$ -chain-associated protein of 70 kD.

CD95 predominantly acts as a death receptor when cross-linked with its CD95 ligand (CD95L) using a well-characterized pathway. Upon ligand binding, Fas-associated death domain associates with CD95, followed by recruitment of the initiator caspase-8 to form the death-inducing signaling complex. Caspase-8 oligomerization initiates its autocatalytic cleavage, followed by the release of active caspase fragments into the cytosol, subsequent activation of effector caspases, DNA fragmentation, and cleavage of cellular substrates (1). Together with the Bcl-2 homology 3-only molecule Bcl-2-interacting mediator of death, the CD95/CD95L system contributes to the deletion of activated T cells during the termination phase of an immune response (2–4). Although the CD95/CD95L system plays a key role in T cell

apoptosis and immunohomeostasis as indicated by the phenotype of lymphoproliferation mice and the induction of autoimmunity and lymphoproliferation in patients with mutations in either the receptor or the ligand (5), CD95 mediates additional functions apart from cell death induction, including amplification of T cell proliferation upon co-stimulation with suboptimal doses of anti-CD3 antibodies (6–8). Nonapoptotic functions of CD95 have also been identified for cells of the central nervous system promoting neuronal development, growth, differentiation, and regeneration (9, 10). CD95 has also been reported to induce tumor growth in lung, thyroid,

© 2009 Strauss et al. This article is distributed under the terms of an Attribution–Noncommercial–Share Alike–No Mirror Sites license for the first six months after the publication date (see <http://www.jem.org/misc/terms.shtml>). After six months it is available under a Creative Commons License (Attribution–Noncommercial–Share Alike 3.0 Unported license, as described at <http://creativecommons.org/licenses/by-nc-sa/3.0/>).

J.A. Lindquist and N. Arhel contributed equally to this paper.

and ovarian cancer, and to trigger basal invasion of glioblastoma in vivo (11–13). T cells inhibited in caspase activation (8) or T cells deficient for Fas-associated death domain (14, 15), caspase-8 (16, 17), or flc-like inhibitory protein (18) exhibited impaired T cell activation and proliferation, suggesting an essential role for molecules downstream of the CD95 pathway in T cell activation.

T cell activation is initiated by binding of the TCR to the appropriate antigen presented by HLA molecules, followed by translocation of the TCR and its associated signaling molecules into lipid rafts, which are microdomains of the plasma membrane enriched in cholesterol and glycosphingolipids. By inducing close proximity of signaling molecules, rafts serve as signaling platforms (19, 20). Src family protein tyrosine kinases (lymphocyte-specific kinase and p59<sup>lck</sup>) subsequently phosphorylate the immunoreceptor tyrosine-based activation motifs of the CD3 chains, followed by recruitment and activation of  $\zeta$ -chain-associated protein of 70 kD (ZAP-70). After phosphorylation by ZAP-70, the transmembrane adaptor linker of activated T cells (LAT) and the cytosolic adaptor protein SLP-76 constitute docking proteins (e.g., for PLC- $\gamma$ ), which then hydrolyzes phosphatidylinositol 3,4-bisphosphate into the secondary messengers inositol 1,4,5-triphosphate and diacylglycerol to initiate  $\text{Ca}^{2+}$  influx and activation of protein kinase C- $\theta$  (PKC- $\theta$ ) and the mitogen activated protein kinase (MAPK) cascade, finally resulting in the activation of transcription through NFAT, NF- $\kappa$ B, and AP-1 (21). In contrast to TCR signaling, the requirement for lipid raft formation in CD95 signaling is controversially debated. Although the association of CD95 with lipid rafts was reported to define the CD95 sensitivity of T cells and to render activated T cells sensitive to apoptosis after TCR stimulation (22), no requirement for raft formation in CD95-mediated death was reported in a B cell line (23). Recent studies, however, suggest that molecules of the CD95 pathway, such as caspase-8 and the c-flc-like inhibitory protein<sub>L</sub>, are essential components of rafts induced after TCR ligation and are associated with NF- $\kappa$ B adaptors during T cell activation (24).

T cell activation and T cell death are tightly controlled processes to guarantee both efficacy of the immune response and prevention of autoimmunity. Whether or not cells undergo apoptosis or start proliferation is defined by cell type, activation status, and co-stimulatory signals. We have previously shown that APCs expressing a membrane-bound form of CD95L (m-CD95L) and the alloantigen HLA-A1 are able to prevent the outgrowth of HLA-A1-specific T cells in long-term T cell stimulation cultures and to efficiently induce apoptosis in pre-activated CD95-expressing T cells (25), suggesting that HLA-A1-specific T cells were deleted after antigen-specific priming by the CD95/CD95L system. In this study, we analyzed the effect of CD95 triggering during the activation of primary human T cells using CD95L-expressing APCs or anti-CD3 and anti-CD28 antibodies together with recombinant CD95L. While activated, CD95-sensitive T cells underwent apoptosis, naive T cells were inhibited in proliferation, and CD95 triggering during T cell priming directly interfered with early proximal TCR

signaling events. We also demonstrate that HIV-1 infection efficiently induced CD95L surface expression in infected macrophages and dendritic cells, and that antigen-loaded, CD95L-expressing macrophages prevent activation of Jurkat cells. Our data suggest a new function of CD95 as a silencer of T cell activation, and CD95L expression on APCs might represent a novel mechanism of viral immune evasion and tolerance induction.

## RESULTS

### m-CD95L-expressing APCs prevent T cell activation and proliferation

CD95 sensitivity in human T cells depends on their activation status. Although naive T cells are CD95 resistant, CD95 sensitivity develops 6–7 d after T cell activation (26). We have previously shown that expression of a noncleavable m-CD95L and HLA-A1 on APCs efficiently prevents development of HLA-A1-specific T cells in long-term T cell cultures in vitro (25). In this study, we analyze whether CD95L-expressing APCs in fact delete antigen-specific T cells or whether CD95 triggering instead prevents antigen-specific T cell priming in naive T cells. Therefore, we stimulated CFSE-labeled HLA-A1<sup>+</sup> T cells with the lymphoblastoid cell line C1R.A1.CD95L expressing the alloantigen HLA-A1 and m-CD95L (25). As controls, we used mock transfectant (C1R.A1.puro; HLA-A1<sup>+</sup> and m-CD95L<sup>−</sup>) or medium. Activation by HLA-A1 in the absence of m-CD95L (C1R.A1.puro) induced T cell proliferation in CD4<sup>+</sup> and CD8<sup>+</sup> T cells starting at day 6. Proliferation of CD4<sup>+</sup> T cells is caused by the expression HLA-Cl II antigens by the stimulator cells. In contrast, the presence of m-CD95L (C1R.A1.CD95L) abolished proliferation in both T cell subsets (Fig. 1 A). Inhibition of proliferation by CD95L was associated with a significant reduction in the expression of activation markers on CD4<sup>+</sup> and CD8<sup>+</sup> T cells at day 6, when the first T cell divisions were detectable (Fig. 1 B). The secretion of the Th1-specific cytokines IFN- $\gamma$  and IL-2 was strongly reduced in the presence of m-CD95L, and secretion of the Th2 cytokine IL-10 was totally impaired in T cells activated with C1R.A1.CD95L after 1, 3, and 5 d compared with T cells stimulated with the mock transfectant (Fig. 1 C). No significant differences were detected for TNF- $\alpha$ . These results demonstrate that the expression of m-CD95L on APCs impairs T cell activation and proliferation.

### Simultaneous triggering of CD95 and TCR induces apoptosis in activated human T cells and inhibits proliferation of naive T cells

HLA-A1-expressing APCs only activate alloantigen-specific T cells, which constitute 3–10% of total T cells. To stimulate T cells independently of antigen specificity, in our experiments we substituted APCs with immobilized anti-CD3 and anti-CD28 antibodies in combination with plate-bound recombinant CD95L. Therefore, CFSE-labeled T cells were stimulated with immobilized anti-CD3 and anti-CD28 antibodies in the absence (CD3/28) or presence of CD95L (CD3/28/95L). After 6 d, proliferation of T cells was efficiently inhibited in the presence of CD95L compared with

CD3/28-stimulated T cells (4 vs. 22%). Triggering of T cells with CD95L alone did not affect proliferation (0%). However, the presence of CD95L-induced apoptosis of 43–47% of nondividing T cells (Fig. 2 A). Thus, the lack of proliferation might be caused by an increase in apoptosis induction.

Because T cells used in this study were purified from human buffy coats and contained on average 30–50% preactivated, CD95-sensitive T cells, constitutive CD95 sensitivity may account for the observed high levels of apoptosis induction. Therefore, we purified naive T cells from the T cell pool by

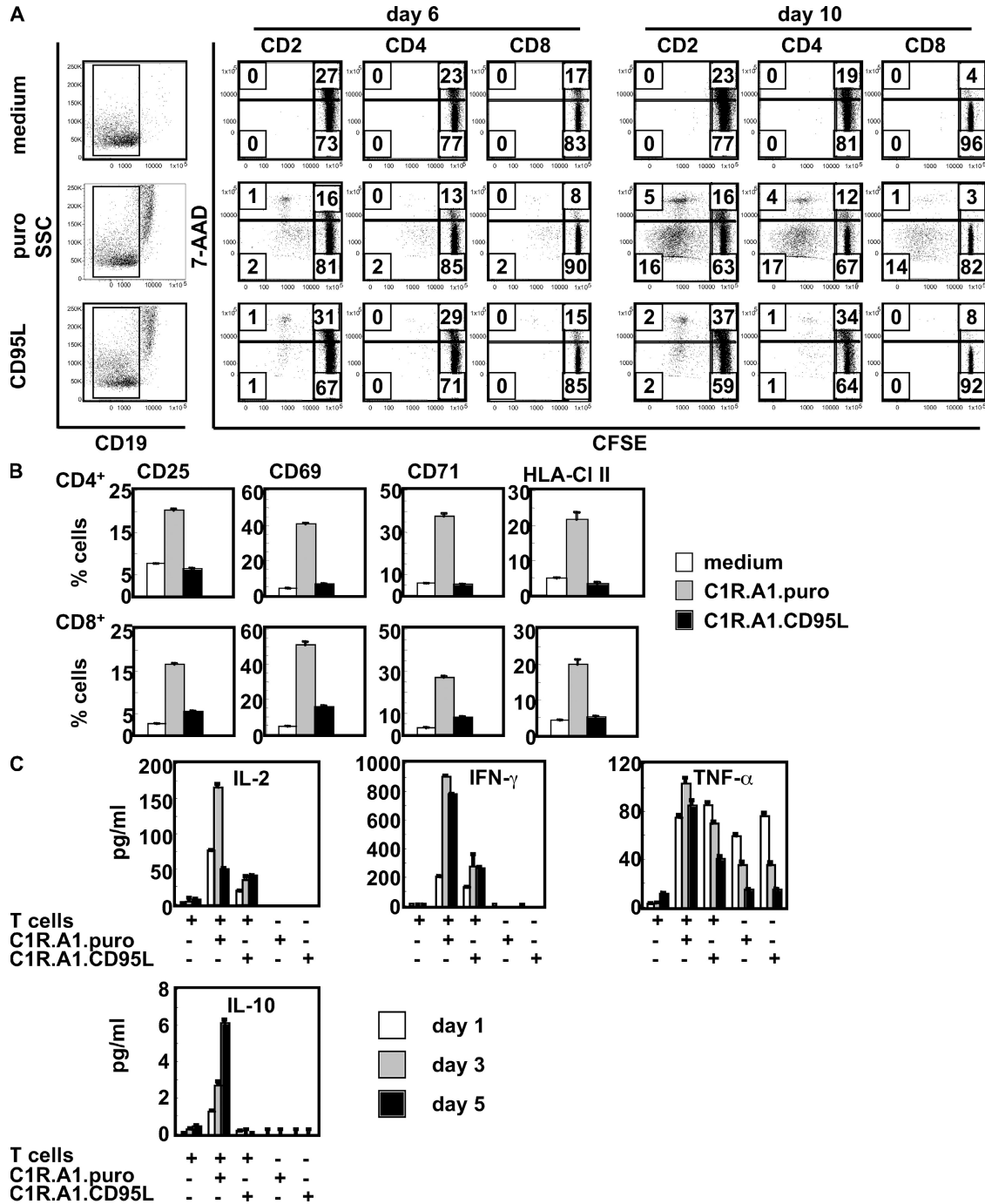


**Figure 1.** m-CD95L-expressing APCs prevent T cell activation and proliferation. Purified CFSE-labeled HLA-A1<sup>+</sup> T cells were stimulated with medium, C1R.A1.puro (puro), or C1R.A1.CD95L (CD95L) cells. (A) After 6 and 10 d, T cells were counterstained for CD19, CD2, CD4, CD8, and 7-AAD. Stimulator cells were excluded by gating on CD19<sup>+</sup> cells and blots represent proliferation and death induction in the different T cell subsets. (B) After 6 d, the expression of activation markers was determined in CD4<sup>+</sup> and CD8<sup>+</sup> T cell subsets. (C) After 1, 3, and 5 d, supernatants were analyzed for cytokine content. Cytokine expression in mitomycin c-treated stimulator cells or T cells alone was used as control. All data are representative of one experiment out of three. Values represent the mean of triplicates  $\pm$  SD.

depleting cells expressing the activation markers CD25 and CD45RO. CFSE-labeled CD45RO<sup>+</sup>CD25<sup>+</sup> T cells showed a significant inhibition of proliferating, live cells in the presence of CD95L compared with T cells stimulated with CD3/28 (CD3/28 = 29% versus CD3/28/95L = 6%), whereas apoptosis induction was only moderately increased (CD3/28 = 8% versus CD3/28/95L = 21%; Fig. 2 B). Although naive T cells are CD95 resistant, they express CD95 on the cell surface; however, at lower levels than compared with activated T cells (Fig. S1). The presence of CD95L during T cell activation prevents secretion of Th1- and Th2-specific cytokines

from naive T cells compared with naive T cells stimulated with CD3/28 alone (Fig. 2 C). To test, whether the efficiency in inhibition of T cell proliferation by CD95L is dependent on the strength of the T cell activating stimulus, we stimulated naive CFSE-labeled T cells with increasing concentrations of immobilized anti-CD3 plus anti-CD28 antibodies. CD95L completely prevented T cell proliferation in CD4<sup>+</sup> and CD8<sup>+</sup> T cells at all antibody concentrations tested (Fig. 3 A). At CD3/38 concentrations of 0.2  $\mu$ g/ml T cells, proliferation is totally inhibited in the presence of CD95L compared with T cells stimulated with CD3/28 (CD2<sup>+</sup>:

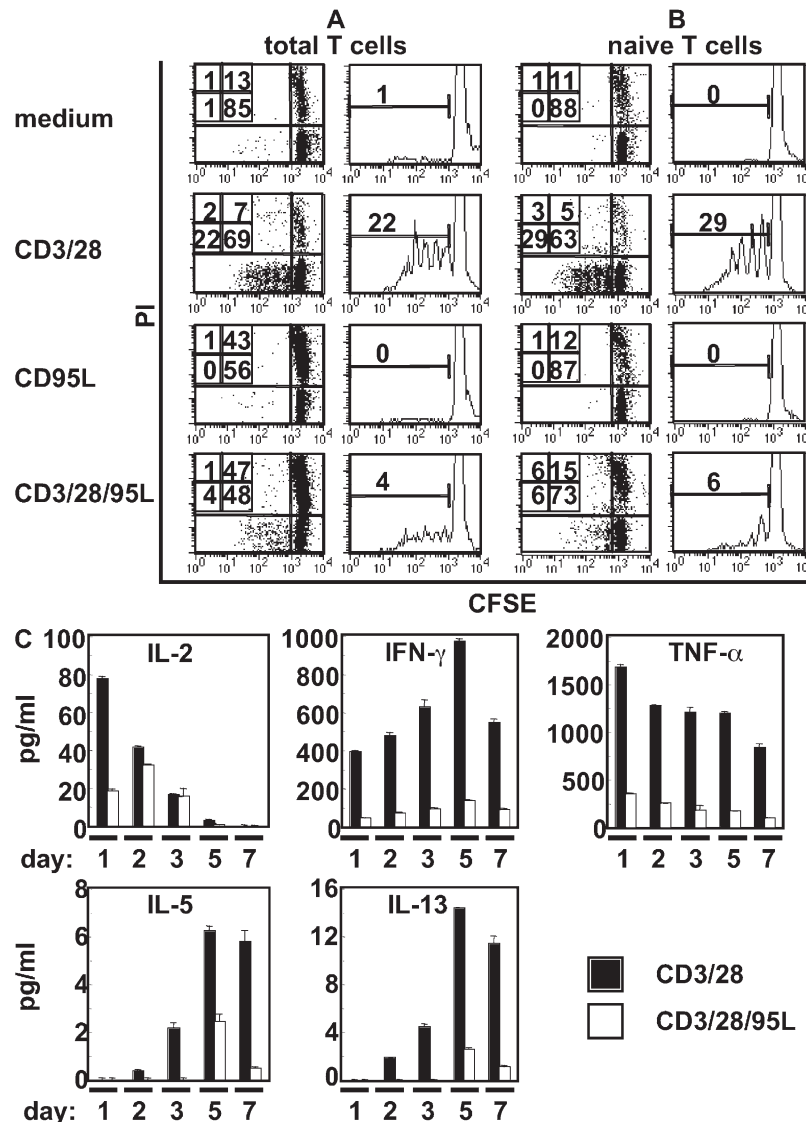


**Figure 2. Simultaneous triggering of CD95 and TCR induces apoptosis in activated T cells and inhibits proliferation and cytokine secretion of naive T cells.** CFSE-labeled purified T cells (total T cells; A) or naive T cells (B) were stimulated with immobilized anti-CD3 and anti-CD28 mAb in the absence (CD3/28) or presence of CD95L (CD3/28/95L) or with medium or CD95L alone. After 6 d, T cells counterstained with PI were analyzed by flow cytometry. The experiment is representative of three experiments carried out. (C) Purified naive T cells were incubated with immobilized anti-CD3 and anti-CD28 mAb in the absence or presence of CD95L. Cytokine secretion was determined in the supernatants at different time points. Secretion of cytokines by T cells cultured in medium or on CD95L-coated plates alone was determined, but expression was below the detection level of the assay (0.5 pg/ml), and therefore not included into the graphs. Data are representative of one experiment out of two carried out. Values present the mean of triplicates  $\pm$  SD.



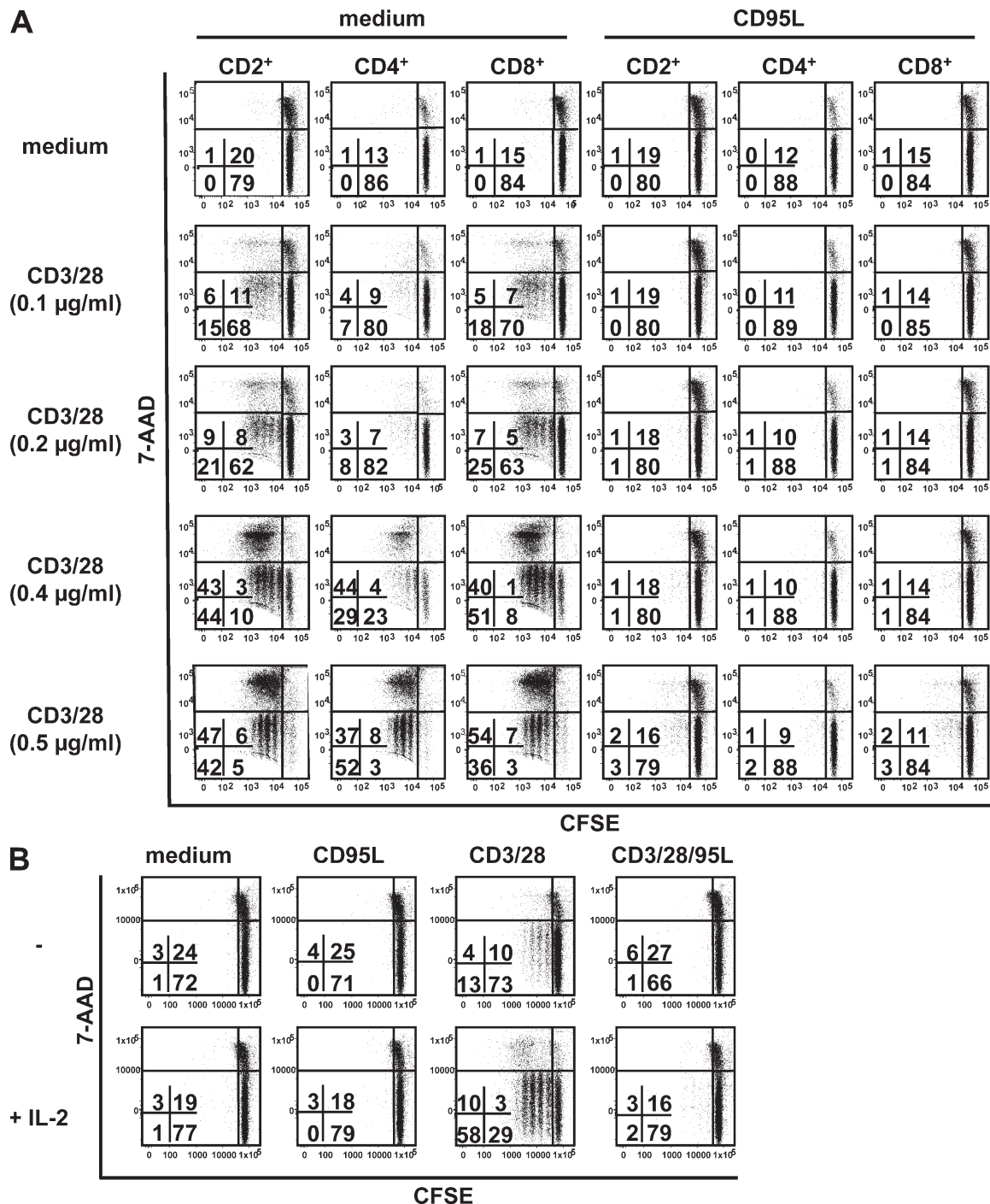


**Figure 3. Independent of the strength of the TCR-mediated signal, proliferation of naive T cells is prevented by CD95 co-stimulation and could not be reverted by IL-2.** (A) CFSE-labeled naive T cells were incubated on plates coated with increasing amounts of anti-CD3 and anti-CD28 antibodies in the absence (medium) or presence of CD95L. After 6 d, T cells were stained for CD2, CD4, CD8, and 7-AAD, and T cell proliferation and death induction were determined in the different T cell subsets. After 6 d of culture, cell recovery was 84% on average in medium-treated cells, 70% in CD95L, 79% in 0.1 µg/ml CD3/28, 102% in 0.2 µg/ml CD3/28, 139% in 0.4 µg/ml CD3/28, 145% in 0.5 µg/ml CD3/28, 77% in 0.1 µg/ml CD3/28 + CD95L, 81% in 0.2 µg/ml CD3/28 + CD95L, 78% in 0.4 µg/ml CD3/28 + CD95L, and 80% in 0.5 µg/ml CD3/28 + CD95L. (B) CFSE-labeled naive T cells were stimulated with immobilized anti-CD3 and anti-CD28 mAb (0.1 µg/ml) (CD3/28) or CD3/28 plus CD95L (CD3/28/95L), or medium or CD95L alone in the presence or absence of recombinant IL-2 (30 U/ml). After 5 d, cells were stained for CD2, and proliferation and cell death induction was determined for CD2<sup>+</sup> T cells. All data are representative of one out of three experiments.

CD3/28 = 30% versus CD3/28/95L = 2%), whereas apoptosis induction was not increased (CD2<sup>+</sup>: CD3/28 = 17% versus CD3/28/95L = 19%). At higher CD3/28 concentrations, dividing T cells probably die because of a limited supply of IL-2, as assays were performed in the absence of exogenous IL-2. First cell divisions were measurable after day 2 of T cell stimulation (unpublished data). Independent of whether isolated CD4<sup>+</sup> and CD8<sup>+</sup> T cells were activated separately or in co-culture, CD95 co-stimulation totally inhibited their proliferation in both culture systems (Fig. S2). Because of the usage of T cells from different donors, we always observed slight differences in proliferation, apoptosis induction, and efficiency of inhibition. However, in all experiments performed, CD95 co-stimulation significantly prevents T cell proliferation between 80 and 100%. Interestingly, adding exogenous recombinant IL-2 could not reverse the inhibitory effect of CD95L on T cell activation. Although the addition of IL-2 efficiently enhanced proliferation in CD3/28-stimulated naive T cells, CD3/28/95L-stimulated T cells did not proliferate irrespective of the presence of IL-2 (Fig. 3 B). No effect of IL-2 was observed in T cells cultured in medium or in the presence of CD95L alone. Membrane-bound CD95L is cleaved by proteases from the cell surface (27), and soluble CD95L might interfere with the antiproliferative effect of immobilized CD95L. However, the addition

of soluble CD95L to our culture system did not prevent the inhibition of T cell proliferation induced by immobilized CD95L (Fig. S3). These results clearly show that T cell priming can be efficiently suppressed by CD95 co-stimulation.

#### CD95 triggering in combination with CD3/28 activation induces T cell unresponsiveness

Because CD95L prevents proliferation of CD3/28-activated naive T cells, we raised the question of whether T cell silencing requires the constitutive presence of CD95L in the T cell stimulation culture. We therefore activated naive T cells with CD3/28, in the absence or presence of CD95L, with CD95L or medium alone. After 6 d,  $2 \times 10^5$  T cells of each stimulation group were analyzed (day 6). The presence of CD95L efficiently prevented T cell proliferation compared with CD3/28-stimulated T cells (Fig. 4). The remaining cells from each stimulation condition were restimulated with immobilized anti-CD3 and -CD28 antibodies in the presence or absence of IL-2, and proliferation was measured 4 d later (day 10). Restimulation of previously CD3/28-activated, medium, or CD95L-stimulated T cells with anti-CD3 and anti-CD28 antibodies induced efficient T cell proliferation (day 10). In contrast, the proliferation of T cells cultured for 6 d in the presence of CD3/28/95L and restimulated with CD3/28 was strongly reduced compared with T cells previously cultured in the

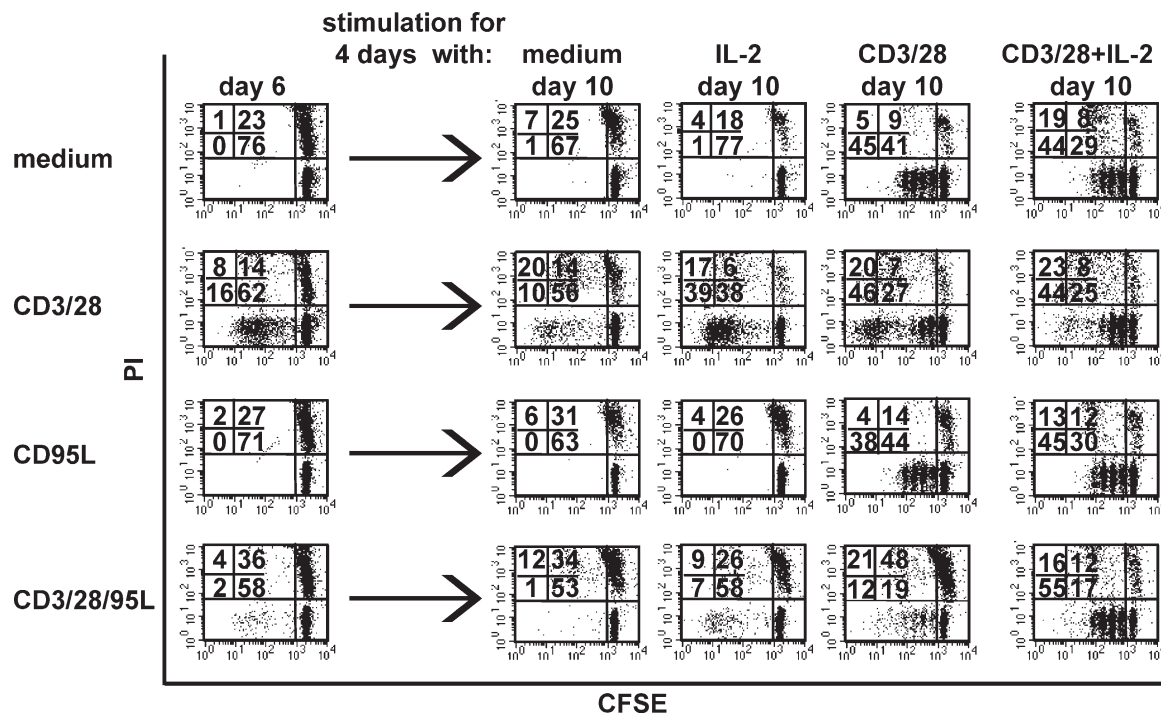


**Figure 4. Co-stimulation of CD95 during T cell priming induces T cell unresponsiveness.** Naive T cells were CFSE labeled and cultured on plates coated with anti-CD3 and anti-CD28 antibodies in the absence (CD3/28) or presence of CD95L (CD3/28/95L) or CD95L alone or medium. After 6 d, T cells were harvested and  $2 \times 10^5$  cells of each stimulation group were stained with propidium iodide (PI) and analyzed by flow cytometry (day 6). The remaining cells from each stimulation group were restimulated on 0.2  $\mu$ g/ml CD3/28-coated plates in the presence or absence of 30 U/ml IL-2 or with 30 U/ml IL-2 alone or left untreated (medium). After 4 d, cells were harvested, stained with PI, and analyzed by flow cytometry (day 10). The experiment is representative for one out of three experiments done.

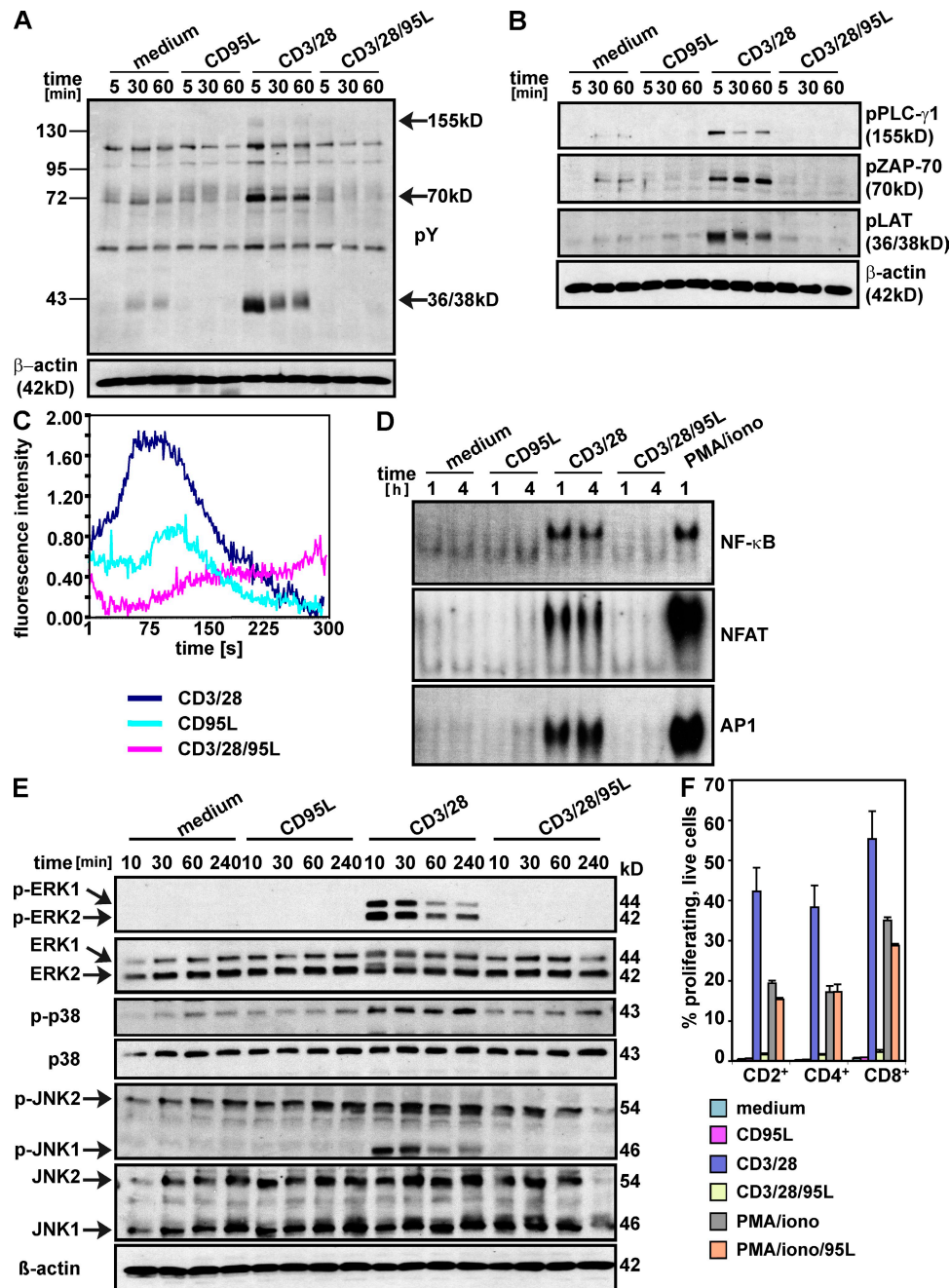


**Figure 5. Inhibition of proximal TCR signaling events in T cells activated in the presence of CD95L.** (A and B) Purified T cells were activated on plates coated with anti-CD3 and anti-CD28 antibodies in the absence or presence of CD95L. Expression of total protein tyrosine phosphorylation (pY; A) or of specific phosphorylated proteins (B) was determined by Western blot analysis at different time points. Arrows indicate differences in protein tyrosine phosphorylation. Experiments were performed three times with similar results. (C) Fluo-4 labeled T cells were seeded on poly-L-lysine-coated slides and antibodies were given to cells directly before the measurement. For measuring the intracellular calcium, a time series of one confocal image plane was recorded. Image acquisition was started immediately after applying the antibodies. After subtracting the background fluorescence, the mean of all cells at each time point was calculated. Each curve represents the mean of three independent experiments. (D) Purified naive T cells were activated with immobilized anti-CD3 plus anti-CD28 antibodies in the presence or absence of CD95L. After 1 and 4 h, nuclear extracts were prepared and analyzed by EMSA for DNA-binding activity of NFAT, AP1, and NF-κB. PMA/ionomycin stimulation served as a positive control. The experiment is representative of three different experiments performed. (E) Purified T cells stimulated with immobilized anti-CD3 and anti-CD28 mAb in the absence or presence of CD95L were lysed after 10, 30, 40, and 240 min, and lysates were subjected to Western blot analysis to determine the expression of phosphorylated and nonphosphorylated MAPKs (ERK1/2, p38, Jnk1/2). β-Actin expression served as a loading control. The experiment shown is representative of two experiments done. (F) CFSE-labeled naive T cells were stimulated with immobilized anti-CD3 and anti-CD28 mAb or with PMA and ionomycin in the absence (CD3/28, PMA/iono) or presence of CD95L (CD3/28/95L, PMA/iono/95L) or with medium or CD95L alone. After 5 d, T cells were stained with 7-AAD, CD2, CD4, and CD8 and analyzed by flow cytometry. Data present the percentage of proliferating, live (7-AAD<sup>-</sup>) T cells in the different T cell subsets. Experiments were performed three times with similar results.

presence of CD95L alone (12 vs. 38%). However, the sustained inhibition of proliferation by CD95L was reversed by the addition of exogenous IL-2. In summary, these data indicate that CD95 co-stimulation of CD3/28-activated naive T cells induces an unresponsive state, which can be overcome by IL-2 after release from CD95L-mediated suppression.

**T cells activated in the presence of CD95L exhibited impaired protein tyrosine phosphorylation,  $\text{Ca}^{2+}$  mobilization, mitogen-activated protein (MAP) kinase activation, and nuclear translocation of transcription factor**

We next estimated whether CD95 co-stimulation would interfere with early signaling events after TCR engagement. After 5 min, CD3/28 stimulation induced a strong tyrosine phosphorylation of proteins with apparent molecular weights of ~150, 70, and 40 kD, respectively, which was still detectable after 60 min and completely blocked in the presence of CD95L (Fig. 5 A). Western blot analysis using phosphospecific antibodies showed that the presence of CD95L during TCR triggering completely abolished the phosphorylation of LAT, ZAP-70, and phospholipase (PLC)- $\gamma$ 1 (Fig. 5 B). Triggering of CD95L alone did not induce protein tyrosine phosphorylation. Because of the lack of protein tyrosine phosphorylation, T cells activated with anti-CD3 and anti-CD28 antibodies in the presence of CD95L showed no  $\text{Ca}^{2+}$  influx compared with T cells activated with CD3/28 (Fig. 5 C). Inhibition of protein tyrosine phosphorylation and decreased  $\text{Ca}^{2+}$ -influx was reflected by impaired nuclear translocation of transcription factors NF- $\kappa$ B, AP1, and NFAT in CD3/28/95L-stimulated T cells compared with CD3/28- or PMA/ionomycin-activated T cells after 1 and 4 h of activation (Fig. 5 D). T cells stimulated with CD95L alone exhibited no differences to untreated T cells. Also, mitogen-activated protein kinase (MAPK) activation known to be induced after TCR stimulation (28) was totally abolished in T cells activated in the presence of CD95L after 10, 30, 60, and 240 min (Fig. 5 E). Although phosphorylation of ERK1/2 and JNK1 was decreased after 30 min in CD3/28-activated samples, phosphorylation of p38 remained constant. Phosphorylation of JNK2 was constitutively independent of the stimulus and CD95L treatment alone did not induce MAPK activation. To further prove that CD95 triggering during T cell activation interferes with proximal T cell receptor events, we activated naive T cells with PMA and ionomycin known to directly activate PKC and  $\text{Ca}^{2+}$  mobilization independent of TCR stimulation. Although CD3/28-mediated T cell proliferation was completely blocked in the presence of CD95L, the proliferation induced by PMA/ionomycin treatment could not be inhibited (Fig. 5 F). In summary, we could show that proximal T cell receptor signaling is severely disabled by CD95 co-stimulation.

**Co-stimulation of CD95 during T cell activation prevents caspase cleavage and formation of a functional signaling platform**

Caspase activity is a hallmark of apoptosis induction, but also a prerequisite for T cell proliferation. CD3/28-mediated

T cell proliferation was abrogated by the broad caspase inhibitor Z-Val-Ala-DL-Asp-fluoromethylketone (z-VAD.fmk; Fig. 6 A). Cleavage of caspase-3, -8, and -10 was detected in CD3/28-stimulated total T cells (pool) or naive T cells isolated from one buffy coat. Surprisingly, the presence of CD95L totally inhibited processing of all caspases examined (Fig. 6 B). No caspase cleavage was detected in T cells stimulated with CD95L alone or medium. To determine caspase activity, naive T cells were incubated for 24 or 48 h with the cell permeable, rhodamine 110-based caspase substrates DEVD (Asp-Glu-Val-Asp; specific for caspase-3, -6, -7, -8, and -10) and Ile-Glu-Thr-Asp (IETD; specific for caspase-8 and granzyme B). The presence of CD95L completely blocked CD3/28-mediated caspase activity at both time points, whereas activation by CD95L alone or medium had no effect (Fig. 6 C). Despite caspase activation in CD3/28-treated T cells, no increase in PARP cleavage compared with untreated cells was observed (Fig. 6 B), suggesting that processed caspases might be sequestered to special membrane compartments during T cell activation to prevent induction of apoptosis. Because TCR-mediated signaling preferentially occurs within lipid rafts, we isolated lipid rafts by discontinuous sucrose gradient from T cells stimulated in the presence or absence of CD95L. Western blot analysis using LAT as a raft marker and the cytoplasmic protein  $\alpha$ -tubulin as a nonraft marker identified fraction 4–6 as raft and fraction 11 as nonraft (Fig. S4). CD3/28-activated T cells exhibited recruitment of PLC- $\gamma$ , PKC- $\theta$ , and ZAP-70 into lipid rafts, whereas nontreated T cells did not. Importantly, triggering CD95 during T cell activation (CD3/28/95L) efficiently prevented recruitment of PLC- $\gamma$ , PKC- $\theta$ , and ZAP-70 into the raft fraction (Fig. 6 D). Untreated T cells and CD95L-treated T cells exhibited no difference in the recruitment of T cell-associated molecules into lipid rafts (Fig. S5). Recruitment of the protein tyrosine phosphatase Scr homology-2 domain-containing phosphatase-1, which is known to be predominantly expressed in cells of the hematopoietic system and to function as a negative regulator of TCR-mediated signaling (29, 30), was not increased in the raft fraction of CD3/28/95L-activated T cells compared with CD3/28-treated T cells. Additionally, Scr homology-2 domain-containing phosphatase-2 was not detectable in the raft fractions independent of the activating stimulus (Fig. 6 E). LAT constitutively expressed in lipid rafts was detected in all raft fractions independent of the stimulation signal. Because caspase-8 is required for T cell and NF- $\kappa$ B activation (16) and active caspases were reported to localize in lipid rafts in activated T cells (24, 31), we determined caspase-8 expression in the lipid raft fractions. The proform of caspase-8 (56/55) was found in all lipid raft fractions independent of the stimulus, whereas the intermediate cleavage product (p43/41) was only found in the raft fraction of CD3/28-activated T cells (Fig. 6 D). In contrast to the finding that the presence of CD95L prevents caspase-8 cleavage (Fig. 6 B), we observed caspase-8 cleavage in the nonraft fraction of CD3/28/95L-stimulated T cells (Fig. 6 D). However, in Fig. 6 D, T cells cultured in medium alone already showed a weak caspase-8 activation, which was not increased in the presence of the CD95L



activation. These differences are caused by varying T cell preparations derived from different donors. Collectively, these results clearly indicate that CD95 triggering during T cell activation prevents the formation of a functional signaling platform.

### CD95L up-regulation on APCs may constitute a mechanism of viral immune evasion

Inhibition of T cell proliferation caused by CD95 triggering during T cell priming may help invading pathogens to avoid

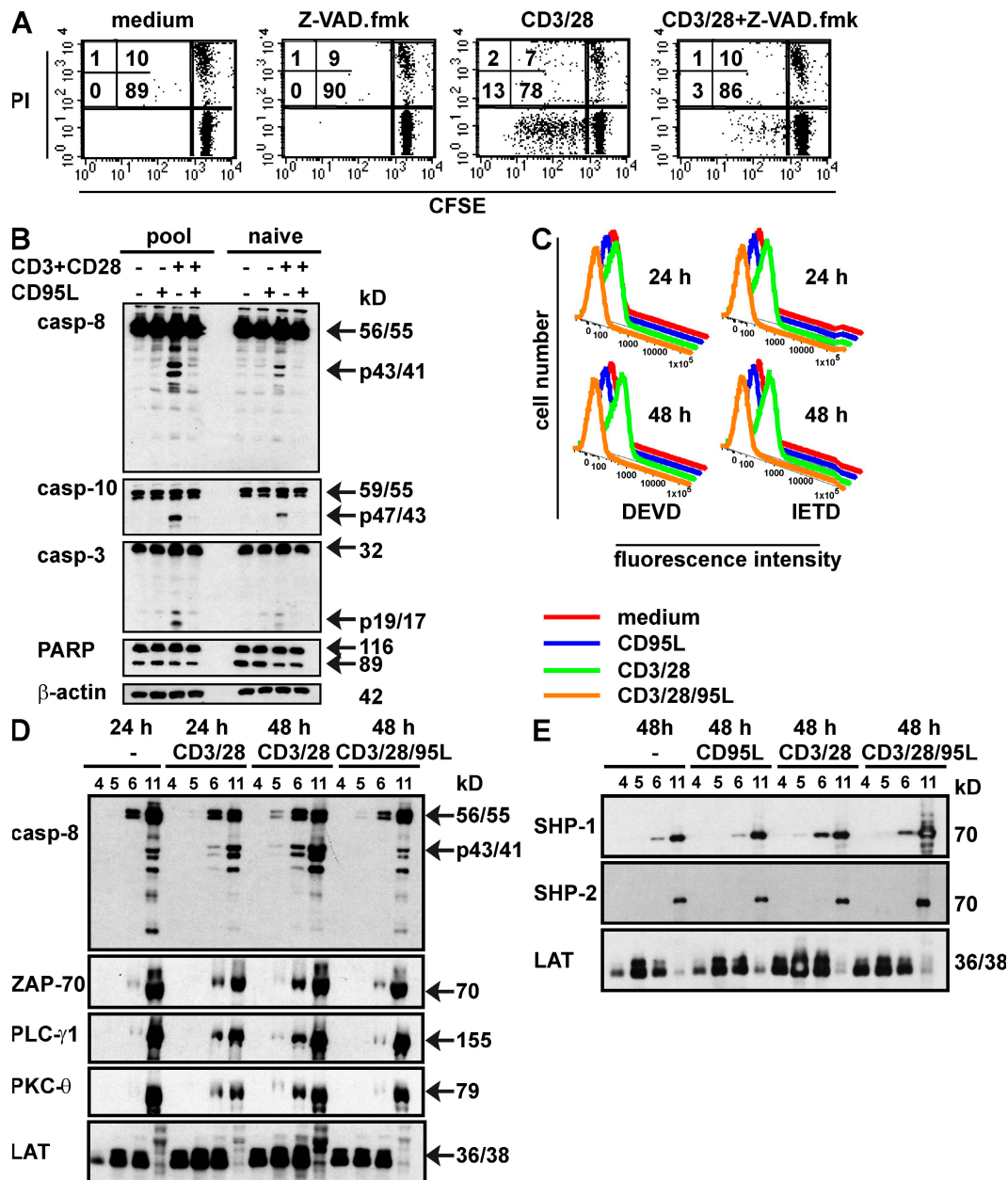


**Figure 6. CD95 triggering during T cell activation prevents caspase activation and translocation of TCR-associated molecules into lipid rafts.** (A) CFSE-labeled naive T cells were activated with immobilized anti-CD3 plus anti-CD28 antibodies (CD3/28) in the presence or absence of Z-VAD.fmk (50  $\mu$ M). After 6 d, cells were stained with propidium iodide (PI) and analyzed by flow cytometry. (B) Purified T cells (pool) and naive T cells (naive) from one buffy coat were activated with immobilized anti-CD3 plus anti-CD28 mAb in the presence or absence of CD95L. After 24 h, cells were harvested and protein lysates were subjected to Western blot analysis.  $\beta$ -Actin served as a loading control. (C) Naive T cells were activated with immobilized anti-CD3 plus anti-CD28 antibody in the absence (CD3/28) or presence of CD95L (CD3/28/95L) or with medium or CD95L alone. After 24 and 48 h, cells were incubated with caspase substrates DEVD-D<sub>2</sub>R and IETD-D<sub>2</sub>R and caspase activity was determined by flow cytometry. (D and E) T cells were activated on anti-CD3 plus anti-CD28-coated plates in the absence (CD3/38) or presence of CD95L (CD3/28/95L) or with CD95L alone or medium. After 24 or 48 h, cells were harvested and lysed, and lysates were separated on a discontinuous sucrose gradient. Proteins from fraction 4–6 (raft fraction) and fraction 11 (nonraft fraction) were analyzed by Western blot analysis. All data shown are representative of three independent experiments.



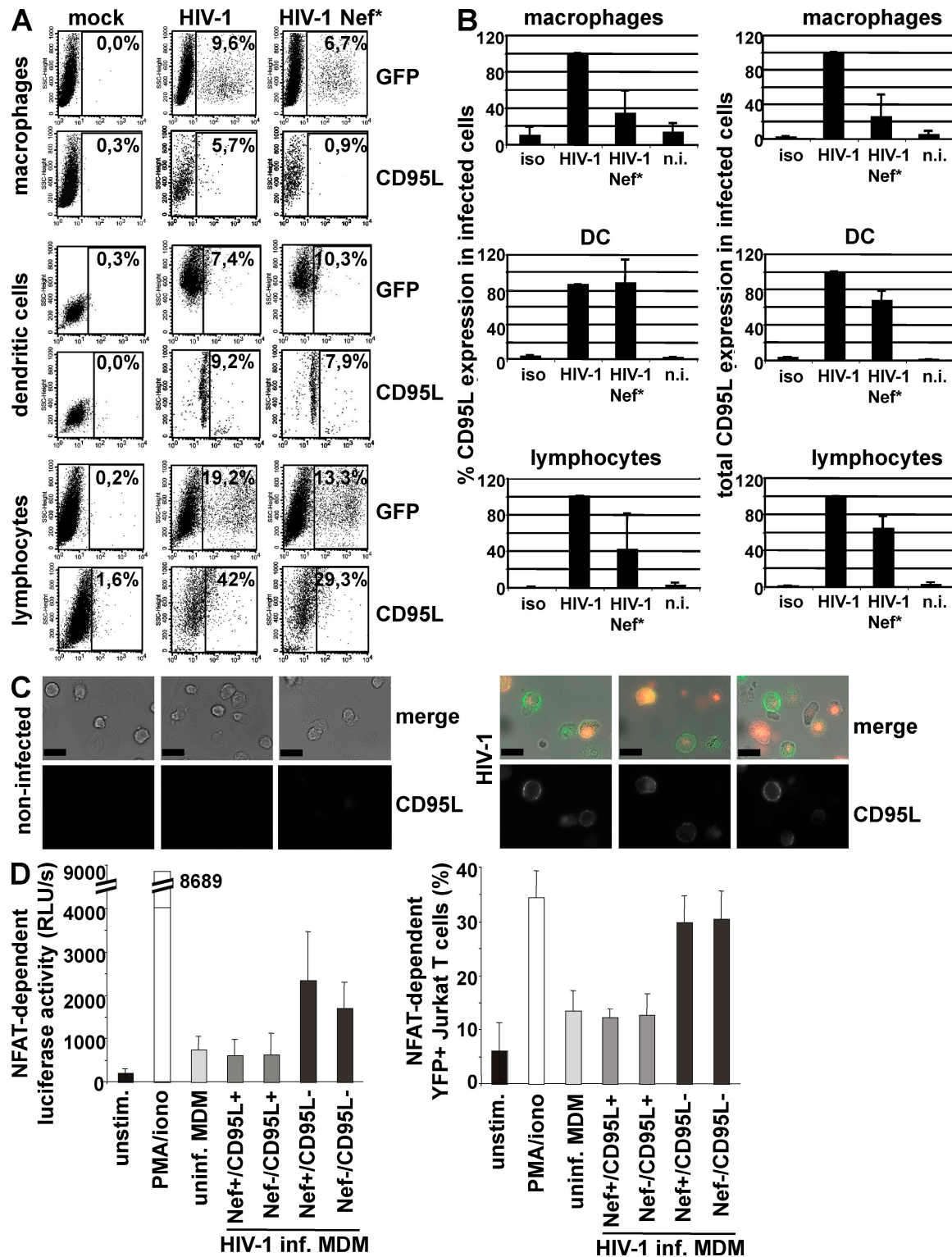


**Figure 7.** HIV-1 infection induces CD95L surface expression in APC and lymphocytes and thereby prevents T cell activation. (A) HIV-1 infection of macrophages, DCs, and activated lymphocytes was determined 4–5 d after infection by GFP expression, and CD95L expression was determined on the GFP<sup>+</sup> population for infected cells and on the entire population for noninfected cultures. Results shown are representative of three independent experiments. (B) The percentage of CD95L-expressing cells (left) and the total CD95L expression, defined as the product between percentage of CD95L<sup>+</sup> cells and mean fluorescence intensity (right), was compared for HIV-1 and HIV-1 Nef\*–infected samples, noninfected (n.i.), and isotype control (iso). HIV-1–infected values were set as 100%. Results shown are a mean of three independent experiments  $\pm$  the SD. (C) Monocyte-derived macrophages (MDM)

detection and elimination by the host immune system. It has been previously shown that the accessory HIV-1 Nef protein, which is required for effective viral persistence and greatly accelerates progression to AIDS (32), induces CD95L expression on T cells (33). HIV-1 also infects macrophages and DCs. Thus, Nef-mediated up-regulation of CD95L on APCs to suppress T cell responses might represent a novel mechanism by which HIV-1 ensures immune evasion. To assess this possibility, we determined the effect of wild-type and Nef-defective HIV-1 infection on surface CD95L expression in macrophages and DCs. Monocyte-derived macrophages, DCs, and lymphocytes were obtained from healthy blood donors and characterized for phenotypic markers immediately before infection (Fig. S6). Uninfected cells (mock) or cells infected with HIV-1 constructs expressing eGFP alone (Nef-deleted HIV-1 Nef<sup>Δ</sup>) or together with Nef (wild-type HIV-1) were examined for CD95L surface expression 4–5 d after infection. Infection rates were typically between 10 and 20% (Fig. 7 A). CD95L surface expression was determined on GFP<sup>+</sup> HIV-1-infected cells. For all three cell types, HIV-1 infection consistently enhanced both the percentage of CD95L-expressing cells and the levels of cell surface expression by up to two orders of magnitude (Fig. 7 B). Nef significantly contributed to induction of CD95L expression in macrophages and lymphocytes, but not so in DCs (Fig. 7 B). To directly determine whether HIV-induced up-regulation of CD95L on the surface of APCs suppresses their capability to stimulate T cells, we examined the effect of CD95L<sup>+</sup> and CD95L<sup>−</sup> macrophages on NFAT activation in two different Jurkat lines containing either the YFP (Jurkat-NFAT-YFP) or the luciferase (Jurkat-NFAT-Luc) reporter genes under the control of an NFAT-dependent promoter. Both T cell lines express a functional TCR and can be stimulated by staphylococcal enterotoxin E (SEE) superantigen. This allowed us to measure both the overall levels of luciferase activity by plate luminometry as well as the proportion of activated YFP<sup>+</sup> T cells by flow cytometry. To avoid crossover between GFP and YFP fluorescences, we infected macrophages with HIV-1 IRES-mCherry viruses and verified HIV infection-induced CD95L expression by fluorescent microscopy (Fig. 7 C). After sorting the infected macrophages into CD95L<sup>+</sup> and CD95L<sup>−</sup> populations and loading with SEE superantigen, we found that HIV-1-infected CD95L<sup>−</sup> macrophages caused approximately two- to threefold higher levels of T cell activation compared with noninfected macrophages (Fig. 7 D). In strict contrast, co-culture with CD95L<sup>+</sup>-infected macrophages resulted in levels of NFAT activation similar to those observed with uninfected macrophages in both readout systems and irrespective of Nef expression. Thus,

HIV-induced CD95L expression on the surface of macrophages clearly suppresses their ability to stimulate T cells. These results suggest that the up-regulation of CD95L on APCs by HIV-1 to silence T cell activation may suppress immune responses, facilitate viral immune evasion, and play a role in the pathogenesis of AIDS.

## DISCUSSION

CD95, which was originally characterized as a death receptor inducing apoptosis after CD95L binding, is now increasingly recognized as a surface receptor with additional functions apart from cell death induction depending on cell type, stimulation, and cellular environment. In this study, we demonstrate for the first time that co-stimulation of CD95 during T cell activation induces inhibition of T cell proliferation in naive T cells by interfering with proximal TCR signaling events, and that CD95 can act as a silencer of the immune response. This novel role of CD95 in down-modulating T cell responses was determined in two different systems: (a) an antigen-specific system using APCs expressing HLA-A1 and m-CD95L to activate HLA-A1<sup>+</sup> T cells and (b) for antigen-independent T cell activation with immobilized CD3 and CD28 antibodies in the presence of recombinant CD95L. The presence of CD95L during T cell activation prevented proliferation of CD4<sup>+</sup> and CD8<sup>+</sup> T cells in both systems. Whereas preactivated CD95-sensitive T cells immediately undergo apoptosis after CD95 stimulation, naive T cells were inhibited in proliferation. These results appear to be in contrast to previous data showing that anti-CD95 antibodies or cross-linked CD95L can augment proliferation of CD3-activated primary human T cells (6, 8). However, in these experiments, T cell activation was suboptimally induced by low concentrations of anti-CD3 antibodies in the absence of co-stimulatory signals, and naive and preactivated T cells were not analyzed separately. Inhibition of T cell activation by CD95L in our system, however, was effective in naive T cells activated in the presence of co-stimulation and was independent of the strength of the activating signal (Fig. 3 A). Although CD95 triggering induces apoptosis in activated T cells, it prevents proliferation during T cell priming in naive T cells, indicating that the time point of CD95 triggering determines the subsequent fate of the T cell. Dependence on the time point of receptor triggering was also reported for signals delivered via CD95L. Although CD95L may promote reverse signaling and T cell co-stimulation directly after antigen-induced CD95L expression, CD95L also mediates apoptosis in T cells at the termination phase of the immune response (34).

T cell activation is initiated by the recognition of antigen through the TCR and subsequent reorganization of signaling

were infected with HIV-1 IRES-mCherry or left uninfected and stained for surface CD95L 4 d later. Images show CD95L staining below and a merge of CD95L (green), mCherry (red), and Nomarski phase contrast above. Bars, 20  $\mu$ m. (D) MDM infected with HIV-1 IRES-mCherry, HIV-1 Nef<sup>Δ</sup> IRES-mCherry were separated at day 4 after infection into CD95L<sup>+</sup> and CD95L<sup>−</sup> MDM and loaded with SEE. The graphs show the extent of T cell activation after co-culture of infected CD95L<sup>+</sup> and CD95L<sup>−</sup> MDM, or uninfected MDM with Jurkat-NFAT-Luc cells (left) or Jurkat-NFAT-YFP (right). 50 ng/ml PMA/1  $\mu$ M ionomycin and unstimulated Jurkat cells serve as positive and negative control. Each graph represents the mean of three independent experiments performed on different blood donors  $\pm$  SD.

molecules into lipid rafts. Although productive T cell activation induced translocation of ZAP-70, PKC- $\theta$ , and PLC- $\gamma$  into lipid rafts, triggering CD95 during T cell activation prevented their recruitment. However, molecules constitutively associated with rafts, such as LAT and lymphocyte-specific kinase (35), were recruited, indicating that CD95 triggering does not induce a global change in raft composition. The mechanism by which CD95 signaling prevents translocation of TCR-associated molecules into the signaling platform remains elusive. Changes in the composition of raft-associated molecules were also observed in anergic T cells, where LAT could not be recruited to lipid rafts because of a selective palmitoylation defect (36), or upon anti-CD4 antibody treatment, which inhibited ZAP-70 translocation into lipid rafts, thereby preventing NF- $\kappa$ B activation (37). Steric hindrance of TCR signaling by recruitment of CD95 into lipid rafts after CD95 co-stimulation did not account for the inhibition of T cell proliferation, as no increase of CD95 in lipid rafts was detected in CD95L-treated T cells (unpublished data). The inhibitory effect of CD95 triggering on T cell activation was also analyzed on downstream events. Thus, protein tyrosine phosphorylation of ZAP-70, LAT, and PLC- $\gamma$ 1 was totally inhibited in the presence of CD95L. We further observed a significant decrease in  $\text{Ca}^{2+}$ -mobilization and inefficient nuclear translocation of transcription factors NF- $\kappa$ B, AP-1, and NFAT in T cells triggered by CD95 during T cell activation. Impaired activation of NF- $\kappa$ B, AP-1, and NFAT was confirmed by the reduced expression of activation markers and a decrease in cytokine secretion. CD95 co-stimulation during T cell priming also prevents MAPK and caspase activation, both known to be required for efficient T cell activation (8, 28). Block of calcium channel,  $\text{Ca}^{2+}$  mobilization, and NFAT activation caused by activation of acidic sphingomyelinase and ceramide release was also observed in T cells stimulated by CD95 alone (38).

Our data add a new function to the already known role of CD95 in apoptosis induction and T cell proliferation (7) by defining CD95 as a T cell silencer. The newly identified immunosuppressive function of CD95 co-stimulation might point to a role of elevated CD95L serum levels in several types of cancers (39–41) or might explain the requirement for CD95L expression on veto cells (42). In the murine system, CD95L expression on veto cells was predominantly correlated with apoptosis induction of CD95<sup>+</sup> T cell precursors (42–44). However, whereas naive murine T cells are constitutively CD95 sensitive (45), naive human T cells are CD95 resistant (26). Therefore, human veto cells may not only induce apoptosis, but may additionally interfere with T cell activation. Although CD95L is predominantly expressed on T cells and NK cells, expression of CD95L was reported in human immature blood DCs, blood monocytes, or activated Langerhans cells (46, 47). Our findings suggest that CD95L expression on APCs might represent a novel mechanism to silence T cells and to support immune evasion. It is known that the HIV-1 Nef up-regulates CD95L in infected T lymphocytes, possibly to induce apoptosis of bystander cytotoxic T cells (33, 48). It has also been shown that HIV-1 infection leads to CD95L up-regulation in

macrophages (49), although the relevance of this effect and the impact of Nef remained unclear. In this study, we confirmed that HIV infection leads to effective CD95L up-regulation in macrophages and T lymphocytes and show for the first time that this effect is also observed in DCs. Furthermore, we demonstrate that Nef plays an important role in CD95L enhancement in macrophages and T lymphocytes, but not in DCs, and that HIV-induced CD95L expression on macrophages significantly prevents the activation of Jurkat T cells. Thus, up-regulation of CD95L expression on APCs by HIV-1 infection might contribute to viral immune evasion by inhibiting T cell activation and promoting unresponsiveness. This mechanism may also have been adopted by other pathogens. Influenza infection in mice induced the expression of CD95L in lymph node-resident DCs (50) and up-regulation of CD95L was observed in human DCs after human cytomegalovirus infection (51). Interestingly, although human cytomegalovirus-infected CD95L-expressing DCs induced apoptosis in activated T cells, some T cells survived contact with infected DCs and exhibited suppressed proliferation after secondary stimulation in the absence of the virus (51). This is in line with our observation that T cells that have encountered CD95L during T cell priming showed decreased proliferation after restimulation. This unresponsive state was partially reverted by the addition of exogenous IL-2. Interestingly, lack of anergy induction was also reported for CD95-deficient lymphoproliferation mice (52).

On the basis of our findings, we propose a novel role for CD95 in naive T cells as a silencer of T cell activation and proliferation by down-regulation of TCR signaling upon co-stimulation. Virus-induced up-regulation of CD95L on the surface of APCs may suppress immune responses, and thereby support immune evasion and tolerance induction.

## MATERIALS AND METHODS

**Cell culture.** All cell lines were grown in complete RPMI 1640 medium (Invitrogen) supplemented with 10% FCS (Lonza), 2 mM L-glutamine, and 1 mM sodium pyruvate at 37°C in a humidified atmosphere containing 7.5%  $\text{CO}_2$ . Establishment of C1R.A1.puro and C1R.A1.CD95L cells were described previously (25). T cells were cultured in complete RPMI 1640 medium supplemented with 2% FCS.

T cells were isolated from PBMCs of healthy HLA-A1<sup>+</sup> donors by RosetteSep (StemCell Technologies). Institutional ethic committee approved the usage of buffy coats for T cell isolation. Purity varies between 92–97%. Naive T cells were separated from the T cell pool by using anti-CD45RO (Cl. UCHL1) and anti-CD25 (Cl. M-A251; BD) antibodies, and subsequent incubation with Dynabeads goat anti-mouse IgG (Invitrogen). Purity was determined by flow cytometry using CD45RA-FITC (Cl. ALB11; Immunotech) and ranged between 90–97%. For proliferation assays and cytokine assays, plates were coated with 0.1  $\mu\text{g}/\text{ml}$  anti-CD3 (cl. OKT3) and 0.1  $\mu\text{g}/\text{ml}$  anti-CD28 (cl. 15E8). In all other assays, 0.25  $\mu\text{g}/\text{ml}$  OKT3 and 0.25  $\mu\text{g}/\text{ml}$  15E8 were used. To trigger CD95, we used 2  $\mu\text{g}/\text{ml}$  immobilized recombinant CD95L (Alexis Biochemicals) or 2  $\mu\text{g}/\text{ml}$  Fc-CD95L supernatant provided by H. Walczak (Imperial College London, London, UK) (53). For TCR-independent T cell activation, we used 0.8 ng/ml PMA (Calbiochem) and 20 nM ionomycin (Calbiochem). CFSE-labeled HLA-A1<sup>+</sup> T cells were stimulated with medium or mitomycin c-treated C1R.A1.puro or C1R.A1.CD95L cells at a ratio of 1:1.

For HIV infection experiments, monocytes were separated from PBMCs of healthy donors by plastic adherence. PBLs were activated for 3 d with

10  $\mu\text{g}/\text{ml}$  PHA before infection. Monocytes were differentiated into immature DCs by culturing for 5 d with 50 ng/ml recombinant human GM-CSF and 20 ng/ml IL4 (Immunotools) or into macrophages by culturing for 7 d with 50 ng/ml human recombinant GM-CSF alone. Phenotypic characterization before infection was done by flow cytometry using CD3, CD4, HLA-DR, CD14, CD1a, CD80, and CD86 antibodies (BD).

**Virus production and infection.** Wild-type NL43-Nef-IRES-GFP or NL43-Nef-IRES-mCherry (referred to as HIV-1) and Nef-deleted NL43-Nef\*-IRES-GFP or NL43-Nef\*-IRES-mCherry (referred to as HIV-1 Nef\*) viruses were produced by transient calcium phosphate cotransfection of 293T cells with proviral plasmid and an expression plasmid for the vesicular stomatitis envelope glycoprotein following standard protocols. Cell supernatants containing virions were collected at 48 h after transfection and used immediately to infect PBL, immature DCs, or macrophages and replaced after 3 h for monocyte-derived cells (or after 6 h for PBLs) by RPMI medium with the appropriate cytokines.

**Microscopy.** Macrophages grown on glass coverslips were stained for surface CD95L (NOK-1) followed by goat anti-mouse Alexa Fluor 647 (Invitrogen) at 4 dpi and analyzed by Apotome structured illumination fluorescence microscopy using an Axiovert microscope equipped with a Plan-Apochromat 63 $\times$ , NA 1.4, oil objective and a MRm charge-coupled device camera piloted by Axiovision software (all from Carl Zeiss, Inc.).

**Activation of Jurkat-NFAT by HIV-infected macrophages.** Infected macrophages labeled with anti-CD95L mAb (NOK-1) followed by rat anti-mouse microbeads (Miltenyi Biotec) were isolated into CD95L<sup>+</sup> and CD95L<sup>-</sup> populations by MACS according to the manufacturer's instructions. CD95L<sup>+</sup> and CD95L<sup>-</sup> macrophages were loaded with 1  $\mu\text{g}/\text{ml}$  SEE superantigen (Toxin Technology) and placed in co-culture at a 1:2 ratio with Jurkat-NFAT-Luc cells or with Jurkat-NFAT-YFP cells. After 6 h, Jurkat-NFAT-Luc cells were lysed and tested for luciferase by plate bioluminescence using the Promega Luciferase Assay System according to the manufacturer's instructions. Jurkat-NFAT-YFP cells were fixed and analyzed by flow cytometry for YFP expression. Incubation was restricted to a 6-h period to avoid interference with CD95-mediated apoptosis in Jurkat targets.

**Flow cytometry.** In general,  $5 \times 10^5$  cells were stained with the following antibodies: CD25-PE, CD69-PE, CD71-FITC, CD95-FITC, HLA-DR, DP, DQ-FITC, CD95L (NOK-1), CD2-APC, CD3-PE, CD4-PE, CD4-Pacific blue, CD8-PE, CD8-FITC, CD8-PE-Cy-7 (BD), CD4-PE-Cy5.5 (Caltag), and goat anti-mouse F(ab')<sub>2</sub>-PE (Dako). Dead cells were visualized using 1  $\mu\text{g}/\text{ml}$  propidium iodide (Sigma-Aldrich) or 1  $\mu\text{g}/\text{ml}$  7-amino-actinomycin-D (AAD; Sigma-Aldrich). To measure caspase activity fluorometrically, T cells were incubated with a 100- $\mu\text{M}$  solution of the rhodamine 110-based, cell membrane-permeable caspase substrates DEVD or IETD (Invitrogen). Analysis was done on FACScan or LSR II flow cytometer (BD).

**CFSE labeling.**  $2 \times 10^6$  T cells/ml were labeled with 100  $\mu\text{l}$  of 50  $\mu\text{M}$  CFSE (Cell Trace CFSE Cell proliferation kit; Invitrogen) for 10 min at 37°C. Cells were immediately washed 4 times with ice-cold PBS-5% FCS and subsequently used for proliferation assays.

**Measurement of intracellular calcium.** T cells were labeled for 20 min at 37°C with 1  $\mu\text{M}$  Fluo-4 and seeded on poly-L-lysine-coated slides (POLY-PRE slides; Sigma-Aldrich). Nonadherent cells were washed away and antibodies were given to cells directly before the measurement. Recombinant CD95L was preincubated for 15 min at 37°C before adding CD3 and CD28 antibodies. To measure the intracellular calcium increase, we recorded a time series (duration, 6 min; interval, 1 s) of one confocal image plane. Images were acquired with an Infinity multibeam confocal device (Visitron) mounted between an Axiovert 200 and a charge-coupled device camera (Cascade II 512). Fluo-4 was excited with a 488-nm Argon/Krypton laser and detected with a 500–550-nm emission filter. A 10 $\times$  plan Neofluar objective and Metamorph

software were used. For image analysis, the cells were digitally outlined and the mean fluorescence intensity was determined for each cell at each single time point (ImageJ software). After subtracting the background fluorescence, the mean fluorescence intensity of all cells at each time point was determined.

#### Determination of cytokine concentrations in cell culture supernatants.

T cells were cultured in medium alone or activated with stimulator cells at a ratio of 1:1 or with antibodies and recombinant CD95L. Supernatants were collected at the indicated time points and immediately stored at  $-80^\circ\text{C}$ . All supernatants were analyzed simultaneously by Immuned GmbH using Bio-Plex technology.

#### Nuclear protein extraction and electrophoretic mobility shift assay.

Purified T cells were activated with immobilized antibodies and recombinant CD95L or with 10 ng/ml PMA and 500 nM ionomycin for 1 h. Nuclear extracts and electrophoretic mobility shift assays (EMSAs) were performed as previously described (54). For EMSA, the following oligonucleotides were used: NF- $\kappa\text{B}$ , 5'-AGTTGAGGGGACTTCCCAGGC-3' (sense); NF-AT, 5'-TCTAAGAGGAAAATTTTCATG-3' (sense); AP-1, 5'-CGCTTGATGAGTCAGCCCGAA-3' (sense).

**Analysis of protein tyrosine phosphorylation.** Purified T cells were serum starved overnight in complete medium supplemented with 0.5% FCS, and subsequently activated on antibody-coated plates and lysed in 50 mM Hepes, 100 mM NaCl, 1% IGEPAL CA-630, 1% laurylmaltoside, 1 mM PMSF, 5 mM EDTA, 1 mM Na<sub>3</sub>VO<sub>4</sub>, 50 mM NaF, and 10 mM Na<sub>4</sub>O<sub>7</sub>P<sub>2</sub>  $\times$  10 H<sub>2</sub>O for 15 min, and protein lysates were subjected to Western blot analysis.

**Isolation of lipid rafts.** T cells were lysed in 50 mM Hepes, 100 mM NaCl, 3% Brij 58, 1 mM PMSF, 5 mM EDTA, 1 mM Na<sub>3</sub>VO<sub>4</sub>, 50 mM NaF, and 10 mM Na<sub>4</sub>O<sub>7</sub>P<sub>2</sub>  $\times$  10 H<sub>2</sub>O for 10 min on ice. The lysate was mixed 1:1 with ice-cold 80% sucrose diluted in 25 mM MES, 5 mM EDTA, and 150 mM NaCl, transferred to Ultra-Clear centrifuge tubes (Beckman Coulter), and overlaid with ice-cold 30% sucrose, followed by ice-cold 5% sucrose. After centrifugation in a Beckman Coulter SW41 rotor, 40,000 rpm, for 20 h at 4°C, 11 1-ml-fractions were collected and subjected to acetone precipitation.

**Western blot analysis.** Western blot analysis was described previously (55). The following antibodies were used: anti-phosphotyrosine (cl. 4G10), LAT (cl. 2E9) (Millipore), phospho-PLC $\gamma$ 1 (Tyr783), phospho-LAT (Tyr191), phospho-Zap-70 (Tyr319)/Syk (Tyr352), caspase-3, PARP, PLC $\gamma$ 1 (Cell Signaling Technology), ZAP 70 (cl. 29), PKC- $\theta$  (cl. 27), JNK1/JNK2 (G151-666; BD),  $\beta$ -actin (AC-15), ERK-1/ERK2 (Sigma-Aldrich), caspase-8 (12F5; Alexis), caspase-10 (cl. 4C1; MBL), ERK1/2(phospho-Thr202/Tyr204), p38 MAPK (phospho-Thr180/Tyr182; Assay Design), anti-active JNKpAb (Promega), p38 (Stressgen) goat anti-mouse IgG-HRP, goat anti-rabbit IgG -HRP, SH-PTP1 (C-19), and SH-PTP2 (B-1; Santa Cruz Biotechnology, Inc.).

**Online supplemental material.** Fig. S1 compares the expression of CD95L on naive and activated human T cells. Fig. S2 compares inhibition of T cell proliferation by CD95 co-stimulation in CD4<sup>+</sup> and CD8<sup>+</sup> T cells cultured isolated or together. Fig. S3 shows that soluble CD95L could not reverse the inhibitory effect of immobilized CD95L during T cell activation. Fig. S4 shows the expression of LAT and  $\alpha$ -tubulin in fractions derived from discontinuous sucrose gradients. Fig. S5 depicts the expression of TCR-associated molecules in raft and nonraft fractions of unstimulated and CD95L-stimulated T cells. Fig. S6 shows the phenotype of primary macrophages, DC, and lymphocytes before HIV infection. The online supplemental material is available online at <http://www.jem.org/cgi/content/full/jem.20082363/DC1>.

We thank Ingrid Knappe for excellent technical assistance. Jurkat-NFAT-YFP cells were a kind gift of Claire HIVroz.

The authors have no conflicting financial interests.

J.A.L. is a member of MaCS and SYBILLA [EU 7FP].

Submitted: 20 October 2008

Accepted: 27 April 2009



## REFERENCES

- Jin, Z., and W.S. El-Deiry. 2005. Overview of cell death signaling pathways. *Cancer Biol. Ther.* 4:139–163.
- Hutcheson, J., J.C. Scatizzi, A.M. Siddiqui, G.K. Haines III, T. Wu, Q.Z. Li, L.S. Davis, C. Mohan, and H. Perlman. 2008. Combined deficiency of proapoptotic regulators Bim and Fas results in the early onset of systemic autoimmunity. *Immunity*. 28:206–217.
- Weant, A.E., R.D. Michalek, I.U. Khan, B.C. Holbrook, M.C. Willingham, and J.M. Grayson. 2008. Apoptosis regulators bim and fas function concurrently to control autoimmunity and CD8(+) T cell contraction. *Immunity*. 28:218–230.
- Hughes, P.D., G.T. Belz, K.A. Fortner, R.C. Budd, A. Strasser, and P. Bouillet. 2008. Apoptosis regulators fas and bim cooperate in shutdown of chronic immune responses and prevention of autoimmunity. *Immunity*. 28:197–205.
- Bidere, N., H.C. Su, and M.J. Lenardo. 2006. Genetic disorders of programmed cell death in the immune system. *Annu. Rev. Immunol.* 24:321–352.
- Alderson, M.R., R.J. Armitage, E. Maraskovsky, T.W. Tough, E. Roux, K. Schooley, F. Ramsdell, and D.H. Lynch. 1993. Fas transduces activation signals in normal human T lymphocytes. *J. Exp. Med.* 178:2231–2235.
- Budd, R.C. 2002. Death receptors couple to both cell proliferation and apoptosis. *J. Clin. Invest.* 109:437–441.
- Kennedy, N.J., T. Kataoka, J. Tschopp, and R.C. Budd. 1999. Caspase activation is required for T cell proliferation. *J. Exp. Med.* 190:1891–1896.
- Tamm, C., J.D. Robertson, E. Sleeper, M. Enoksson, M. Emgard, S. Orrenius, and S. Ceccatelli. 2004. Differential regulation of the mitochondrial and death receptor pathways in neural stem cells. *Eur. J. Neurosci.* 19:2613–2621.
- Desbarats, J., R.B. Birge, M. Mimouni-Rongy, D.E. Weinstein, J.S. Palerm, and M.K. Newell. 2003. Fas engagement induces neurite growth through ERK activation and p35 upregulation. *Nat. Cell Biol.* 5:118–125.
- Mitsiades, C.S., V. Poulaki, G. Fanourakis, E. Sozopoulos, D. McMillin, Z. Wen, G. Voutsinas, S. Tseloni-Balafouta, and N. Mitsiades. 2006. Fas signaling in thyroid carcinomas is diverted from apoptosis to proliferation. *Clin. Cancer Res.* 12:3705–3712.
- Lee, J.K., T.J. Sayers, T.C. Back, J.M. Wigginton, and R.H. Wiltrot. 2003. Lack of FasL-mediated killing leads to in vivo tumor promotion in mouse Lewis lung cancer. *Apoptosis*. 8:151–160.
- Kleber, S., I. Sancho-Martinez, B. Wiestler, A. Beisel, C. Gieffers, O. Hill, M. Thiemann, W. Mueller, J. Sykora, A. Kuhn, et al. 2008. Yes and PI3K bind CD95 to signal invasion of glioblastoma. *Cancer Cell*. 13:235–248.
- Zhang, J., D. Cado, A. Chen, N.H. Kabra, and A. Winoto. 1998. Fas-mediated apoptosis and activation-induced T-cell proliferation are defective in mice lacking FADD/Mort1. *Nature*. 392:296–300.
- Walsh, C.M., B.G. Wen, A.M. Chinnaiyan, K. O'Rourke, V.M. Dixit, and S.M. Hedrick. 1998. A role for FADD in T cell activation and development. *Immunity*. 8:439–449.
- Su, H., N. Bidere, L. Zheng, A. Cubre, K. Sakai, J. Dale, L. Salmena, R. Hakem, S. Straus, and M. Lenardo. 2005. Requirement for caspase-8 in NF-kappaB activation by antigen receptor. *Science*. 307:1465–1468.
- Salmena, L., B. Lemmers, A. Hakem, E. Matsiyak-Zablocki, K. Murakami, P.Y. Au, D.M. Berry, L. Tamblin, A. Shehabeldin, E. Migon, et al. 2003. Essential role for caspase 8 in T-cell homeostasis and T-cell-mediated immunity. *Genes Dev.* 17:883–895.
- Chau, H., V. Wong, N.J. Chen, H.L. Huang, W.J. Lin, C. Mirtsos, A.R. Elford, M. Bonnard, A. Wakeham, A.I. You-Ten, et al. 2005. Cellular FLICE-inhibitory protein is required for T cell survival and cycling. *J. Exp. Med.* 202:405–413.
- Xavier, R., T. Brennan, Q. Li, C. McCormack, and B. Seed. 1998. Membrane compartmentation is required for efficient T cell activation. *Immunity*. 8:723–732.
- Montixi, C., C. Langlet, A.M. Bernard, J. Thimonier, C. Dubois, M.A. Wurbel, J.P. Chauvin, M. Pierres, and H.T. He. 1998. Engagement of T cell receptor triggers its recruitment to low-density detergent-insoluble membrane domains. *EMBO J.* 17:5334–5348.
- Simeoni, L., M. Smida, V. Posevitz, B. Schraven, and J.A. Lindquist. 2005. Right time, right place: the organization of membrane proximal signaling. *Semin. Immunol.* 17:35–49.
- Muppidi, J.R., and R.M. Siegel. 2004. Ligand-independent redistribution of Fas (CD95) into lipid rafts mediates clonotypic T cell death. *Nat. Immunol.* 5:182–189.
- Algeciras-Schimmich, A., L. Shen, B.C. Barnhart, A.E. Murmann, J.K. Burkhardt, and M.E. Peter. 2002. Molecular ordering of the initial signaling events of CD95. *Mol. Cell. Biol.* 22:207–220.
- Misra, R.S., J.Q. Russell, A. Koenig, J.A. Hinshaw-Makepeace, R. Wen, D. Wang, H. Huo, D.R. Littman, U. Ferch, J. Ruland, et al. 2007. Caspase-8 and c-FLIP associate in lipid rafts with NF-kappaB adaptors during T cell activation. *J. Biol. Chem.* 282:19365–19374.
- Strauss, G., W. Osen, I. Knappe, E.M. Jacobsen, S.M. Muller, and K.M. Debatin. 2007. Membrane-bound CD95 ligand expressed on human antigen-presenting cells prevents alloantigen-specific T cell response without impairment of viral and third-party T cell immunity. *Cell Death Differ.* 14:480–488.
- Klas, C., K.M. Debatin, R.R. Jonker, and P.H. Krammer. 1993. Activation interferes with the APO-1 pathway in mature human T cells. *Int. Immunol.* 5:625–630.
- Askenasy, N., E.S. Yolcu, I. Yaniv, and H. Shirwan. 2005. Induction of tolerance using Fas ligand: a double-edged immunomodulator. *Blood*. 105:1396–1404.
- Zhang, Y.L., and C. Dong. 2005. MAP kinases in immune responses. *Cell. Mol. Immunol.* 2:20–27.
- Kosugi, A., J. Sakakura, K. Yasuda, M. Ogata, and T. Hamaoka. 2001. Involvement of SHP-1 tyrosine phosphatase in TCR-mediated signaling pathways in lipid rafts. *Immunity*. 14:669–680.
- Neel, B.G., H. Gu, and L. Pao. 2003. The 'Shp'ing news: SH2 domain-containing tyrosine phosphatases in cell signaling. *Trends Biochem. Sci.* 28:284–293.
- Koenig, A., J.Q. Russell, W.A. Rodgers, and R.C. Budd. 2008. Spatial differences in active caspase-8 defines its role in T-cell activation versus cell death. *Cell Death Differ.* 15:1701–1711.
- Kirchhoff, F., M. Schindler, A. Specht, N. Arhel, and J. Munch. 2008. Role of Nef in primate lentiviral immunopathogenesis. *Cell. Mol. Life Sci.* 65:2621–2636.
- Xu, X.N., B. Laffert, G.R. Screaton, M. Kraft, D. Wolf, W. Kolanus, J. Mongkolsapay, A.J. McMichael, and A.S. Baur. 1999. Induction of Fas ligand expression by HIV involves the interaction of Nef with the T cell receptor zeta chain. *J. Exp. Med.* 189:1489–1496.
- Suzuki, I., and P.J. Fink. 2000. The dual functions of fas ligand in the regulation of peripheral CD8+ and CD4+ T cells. *Proc. Natl. Acad. Sci. USA*. 97:1707–1712.
- Drevot, P., C. Langlet, X.J. Guo, A.M. Bernard, O. Colard, J.P. Chauvin, R. Lasserre, and H.T. He. 2002. TCR signal initiation machinery is pre-assembled and activated in a subset of membrane rafts. *EMBO J.* 21:1899–1908.
- Hundt, M., H. Tabata, M.S. Jeon, K. Hayashi, Y. Tanaka, R. Krishna, L. De Giorgio, Y.C. Liu, M. Fukata, and A. Altman. 2006. Impaired activation and localization of LAT in anergic T cells as a consequence of a selective palmitoylation defect. *Immunity*. 24:513–522.
- Chentouf, M., S. Ghannam, C. Bes, S. Troade, M. Cerutti, and T. Chardes. 2007. Recombinant anti-CD4 antibody 13B8.2 blocks membrane-proximal events by excluding the Zap70 molecule and downstream targets SLP-76, PLC gamma 1, and Vav-1 from the CD4-segregated Brij 98 detergent-resistant raft domains. *J. Immunol.* 179:409–420.
- Leppl-Wienhues, A., C. Belka, T. Laun, A. Jekle, B. Walter, U. Wieland, M. Welz, L. Heil, J. Kun, G. Busch, et al. 1999. Stimulation of CD95 (Fas) blocks T lymphocyte calcium channels through sphingomyelinase and sphingolipids. *Proc. Natl. Acad. Sci. USA*. 96:13795–13800.
- Mizutani, Y., F. Hongo, N. Sato, O. Ogawa, O. Yoshida, and T. Miki. 2001. Significance of serum soluble Fas ligand in patients with bladder carcinoma. *Cancer*. 92:287–293.
- Taylor, D.D., C. Gercel-Taylor, K.S. Lyons, J. Stanson, and T.L. Whiteside. 2003. T-cell apoptosis and suppression of T-cell receptor/CD3-zeta by Fas ligand-containing membrane vesicles shed from ovarian tumors. *Clin. Cancer Res.* 9:5113–5119.
- Tsutsumi, S., H. Kuwano, T. Shimura, N. Morinaga, E. Mochiki, and T. Asao. 2000. Circulating soluble Fas ligand in patients with gastric carcinoma. *Cancer*. 89:2560–2564.



42. Reich-Zeliger, S., Y. Zhao, R. Krauthgamer, E. Bachar-Lustig, and Y. Reisner. 2000. Anti-third party CD8<sup>+</sup> CTLs as potent veto cells: coexpression of CD8 and FasL is a prerequisite. *Immunity*. 13:507–515.
43. Rich, R.F., and W.R. Green. 1999. Antiretroviral cytolytic T-lymphocyte nonresponsiveness: FasL/Fas-mediated inhibition of CD4(+) and CD8(+) antiviral T cells by viral antigen-positive veto cells. *J. Virol.* 73:3826–3834.
44. Reich-Zeliger, S., J. Gan, E. Bachar-Lustig, and Y. Reisner. 2004. Tolerance induction by veto CTLs in the TCR transgenic 2C mouse model. II. Deletion of effector cells by Fas-Fas ligand apoptosis. *J. Immunol.* 173:6660–6666.
45. Suda, T., M. Tanaka, K. Miwa, and S. Nagata. 1996. Apoptosis of mouse naive T cells induced by recombinant soluble Fas ligand and activation-induced resistance to Fas ligand. *J. Immunol.* 157:3918–3924.
46. Lu, G., B.M. Janjic, J. Janjic, T.L. Whiteside, W.J. Storkus, and N.L. Vujanovic. 2002. Innate direct anticancer effector function of human immature dendritic cells. II. Role of TNF, lymphotoxin- $\alpha$ (1) $\beta$ (2), Fas ligand, and TNF-related apoptosis-inducing ligand. *J. Immunol.* 168:1831–1839.
47. De Panfilis, G., M. Venturini, A. Lavazza, M.A. Mommaas, D. Semenza, C. Torresani, and G. Pasolini. 2003. The tolerogenic molecule CD95-L is expressed on the plasma membrane of human activated, but not resting, Langerhans' cells. *Exp. Dermatol.* 12:692–699.
48. Baumler, C.B., T. Bohler, I. Herr, A. Benner, P.H. Krammer, and K.M. Debatin. 1996. Activation of the CD95 (APO-1/Fas) system in T cells from human immunodeficiency virus type-1-infected children. *Blood*. 88:1741–1746.
49. Dockrell, D.H., A.D. Badley, J.S. Villacian, C.J. Heppelmann, A. Algeciras, S. Ziesmer, H. Yagita, D.H. Lynch, P.C. Roche, P.J. Leibson, and C.V. Paya. 1998. The expression of Fas Ligand by macrophages and its upregulation by human immunodeficiency virus infection. *J. Clin. Invest.* 101:2394–2405.
50. Legge, K.L., and T.J. Braciale. 2005. Lymph node dendritic cells control CD8<sup>+</sup> T cell responses through regulated FasL expression. *Immunity*. 23:649–659.
51. Raftery, M.J., M. Schwab, S.M. Eibert, Y. Samstag, H. Walczak, and G. Schonrich. 2001. Targeting the function of mature dendritic cells by human cytomegalovirus: a multilayered viral defense strategy. *Immunity*. 15:997–1009.
52. Bosu, P., G.G. Singer, P. Andres, R. Ettinger, A. Marshak-Rothstein, and A.K. Abbas. 1993. Mature CD4<sup>+</sup> T lymphocytes from MRL/lpr mice are resistant to receptor-mediated tolerance and apoptosis. *J. Immunol.* 151:7233–7239.
53. Geserick, P., C. Drewniok, M. Hupe, T.L. Haas, P. Diessenbacher, M.R. Sprick, M.P. Schon, F. Henkler, H. Gollnick, H. Walczak, and M. Leverkus. 2008. Suppression of cFLIP is sufficient to sensitize human melanoma cells to TRAIL- and CD95L-mediated apoptosis. *Oncogene*. 27:3211–3220.
54. Kasperczyk, H., K. La Ferla-Bruhl, M.A. Westhoff, L. Behrend, R.M. Zwacka, K.M. Debatin, and S. Fulda. 2005. Betulinic acid as new activator of NF- $\kappa$ B: molecular mechanisms and implications for cancer therapy. *Oncogene*. 24:6945–6956.
55. Strauss, G., M.A. Westhoff, P. Fischer-Posovszky, S. Fulda, M. Schanbacher, S.M. Eckhoff, K. Stahnke, N. Vahsen, G. Kroemer, and K.M. Debatin. 2008. 4-hydroperoxy-cyclophosphamide mediates caspase-independent T-cell apoptosis involving oxidative stress-induced nuclear relocation of mitochondrial apoptogenic factors AIF and EndoG. *Cell Death Differ.* 15:332–343.

## SUPPLEMENTAL MATERIAL

Strauss et al., <http://www.jem.org/cgi/content/full/jem.20082363/DC1>

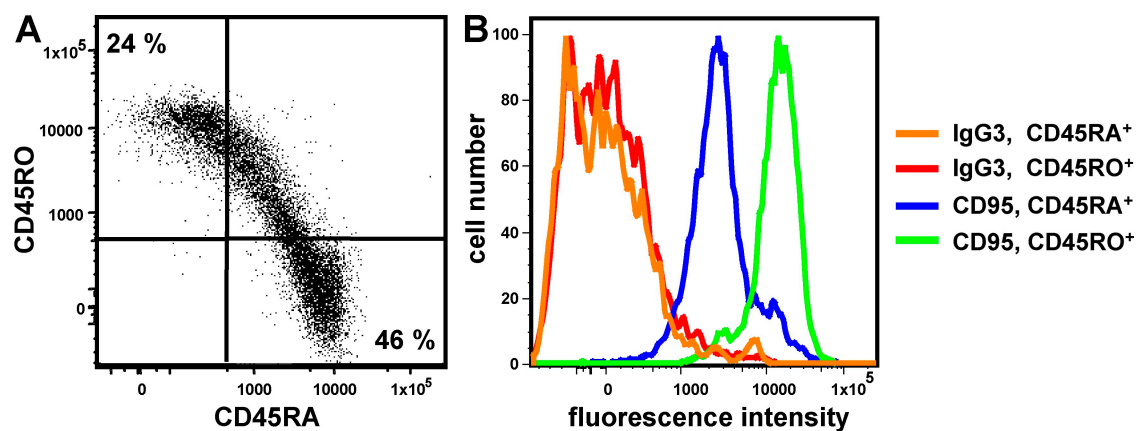


**Figure S1.** CD95 is up-regulated on preactivated, CD45RO<sup>+</sup> T cells. Purified T cells isolated from a buffy coat of a healthy donor were stained with CD45RA-FITC, CD45RO-PE (A), and APO-1 (anti-CD95) supernatant or IgG3 isotype control, followed by biotinylated polyclonal rabbit anti-mouse F(ab)<sub>2</sub> and streptavidin-APC. Cells were counterstained with 7-AAD to gate on live cells. Expression of CD95 and IgG3 is shown on the CD45RA<sup>+</sup> and CD45RO<sup>+</sup> T cell population (B). Experiment is representative of two experiments carried out with T cells from different donors.

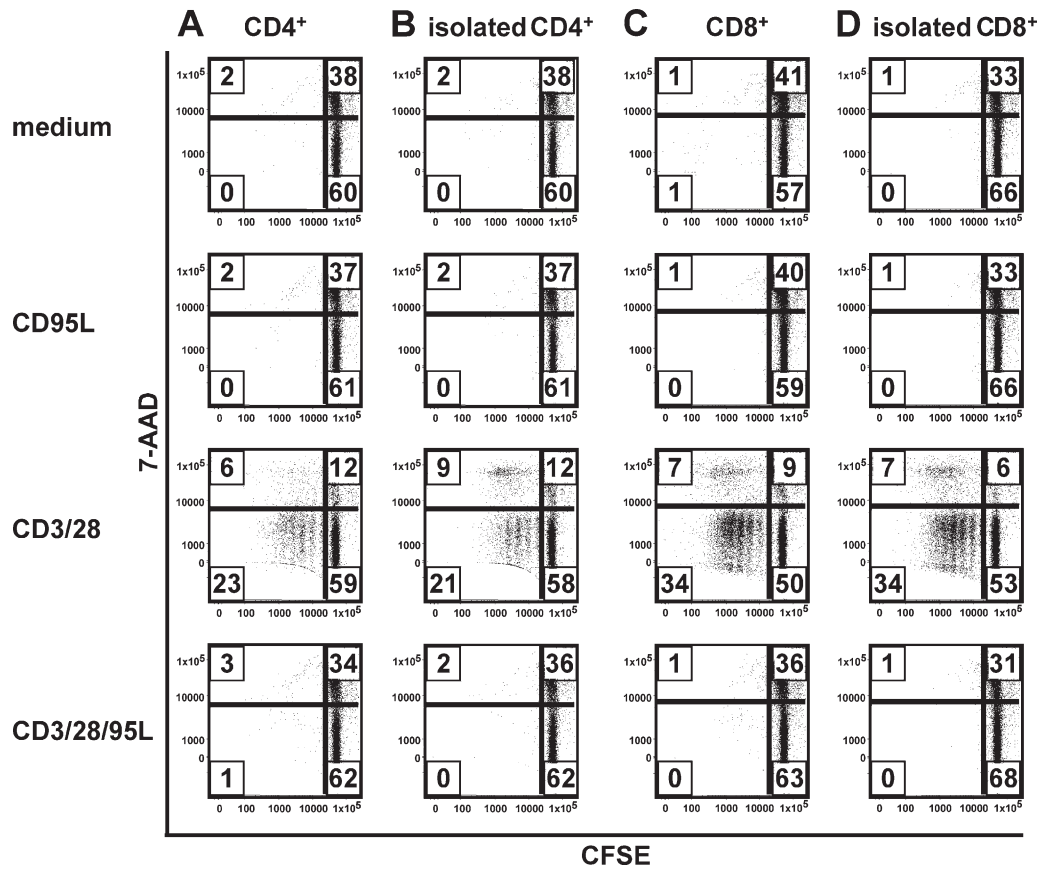


**Figure S2. Costimulation of CD95 blocks T cell proliferation in isolated and co-cultured CD4<sup>+</sup> and CD8<sup>+</sup> T cell subsets.** Naive T cells were isolated from a buffy coat of a healthy donor. Subsequently, CD4<sup>+</sup> and CD8<sup>+</sup> T cells were isolated from total, naive T cells by incubation with OKT8 (anti-CD8) supernatant to obtain CD4<sup>+</sup> T cells or HP2/6 (anti-CD4) supernatant to obtain CD8<sup>+</sup> T cells, followed by treatment with goat anti-mouse IgG magnetic beads. Total T cells (A and C) and isolated CD4<sup>+</sup> (B) and CD8<sup>+</sup> (D) T cells were CFSE labeled and stimulated with immobilized anti-CD3 plus anti-CD28 antibody (0.2  $\mu$ g/ml) in the absence (CD3/28) or presence (CD3/28/95L) of CD95L or with CD95L or medium alone. After 6 d, naive T cells were stained with CD4-Pacific blue; CD8-PE-Cy7, the isolated CD4<sup>+</sup> T cells, were stained with CD4-Pacific blue; and isolated CD8<sup>+</sup> T cells were stained with CD8-PE-Cy7. Proliferation and cell death in total naive T cells was determined by gating on CD4<sup>+</sup> (A) and CD8<sup>+</sup> (C) T cells and compared with isolated CD4<sup>+</sup> (B) and isolated CD8<sup>+</sup> (D) T cells. This experiment is representative of two experiments.

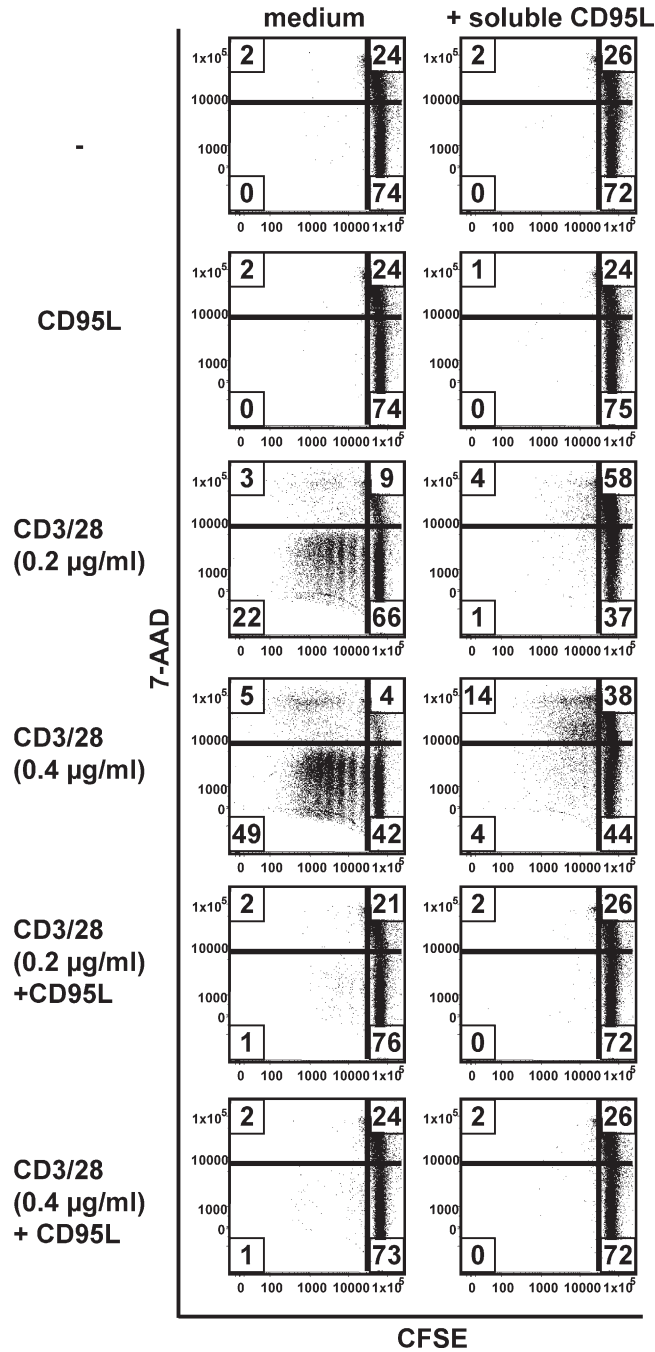


**Figure S3.** Soluble CD95L does not reverse the antiproliferative effect of immobilized CD95L during T cell activation. CFSE-labeled naive T cells were activated with immobilized anti-CD3 and anti-CD28 antibodies (CD3/28), immobilized CD95L (CD95L; 2 µg/ml), and immobilized CD3/28 + immobilized CD95L (CD3/28 + CD95L) or left untreated (-) in the absence (medium) or presence of soluble CD95L (2 µg/ml). After 6 d, cells were harvested and stained with CD2-APC and 7-AAD, and proliferation and apoptosis induction were analyzed in the CD2<sup>+</sup> population. Experiment is representative of two experiments.

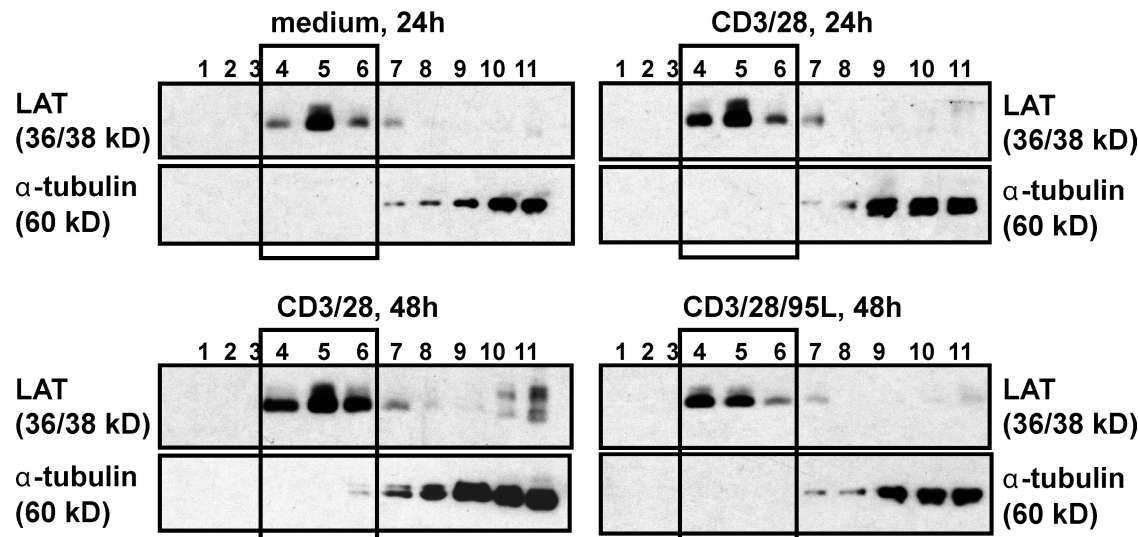


**Figure S4.** Determination of the raft and nonraft fraction of stimulated T cells after discontinuous sucrose gradient. Purified T cells isolated from a buffy coat of a healthy donor were left untreated (medium) or activated with immobilized anti-CD3 and -CD28 antibodies in the absence (CD3/28) or presence (CD3/28/95L) of CD95L for 24 or 48 h. Subsequently,  $5 \times 10^7$  T cells were lysed and lysates were loaded on a discontinuous sucrose gradient. 11 1-ml fractions were collected after 20 h of centrifugation and 25  $\mu$ l of each fraction was immediately subjected to Western blot analysis. Gels were stained for the raft marker LAT and the cytoplasmic protein  $\alpha$ -tubulin (DM1A). The experiment is representative of three independent experiments.

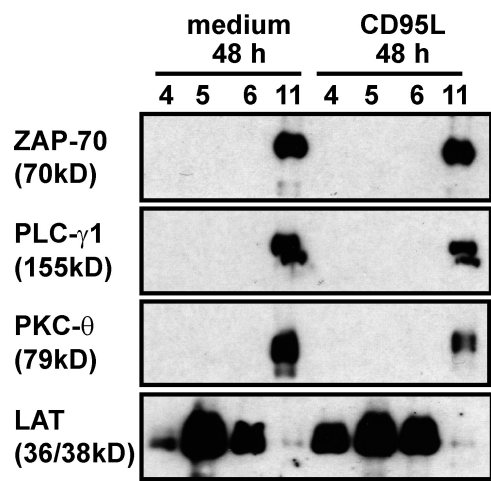


**Figure S5.** Untreated and CD95L-treated T cells do not exhibit differences in the recruitment of TCR-associated signal molecules into lipid rafts. Purified T cells isolated from a buffy coat of a healthy donor were left untreated (medium) or were stimulated in the presence of CD95L for 48 h. Precipitated raft (4–6) and nonraft fractions (Mitsiades, C.S., V. Poulaki, G. Fanourakis, E. Sotopoulos, D. McMillin, Z. Wen, G. Voutsinas, S. Tseleni-Balafouta, and N. Mitsiades. 2006. *Clin. Cancer Res.* 12:3705–3712) were subjected to Western blot analysis. The results are representative for one experiment out of two.



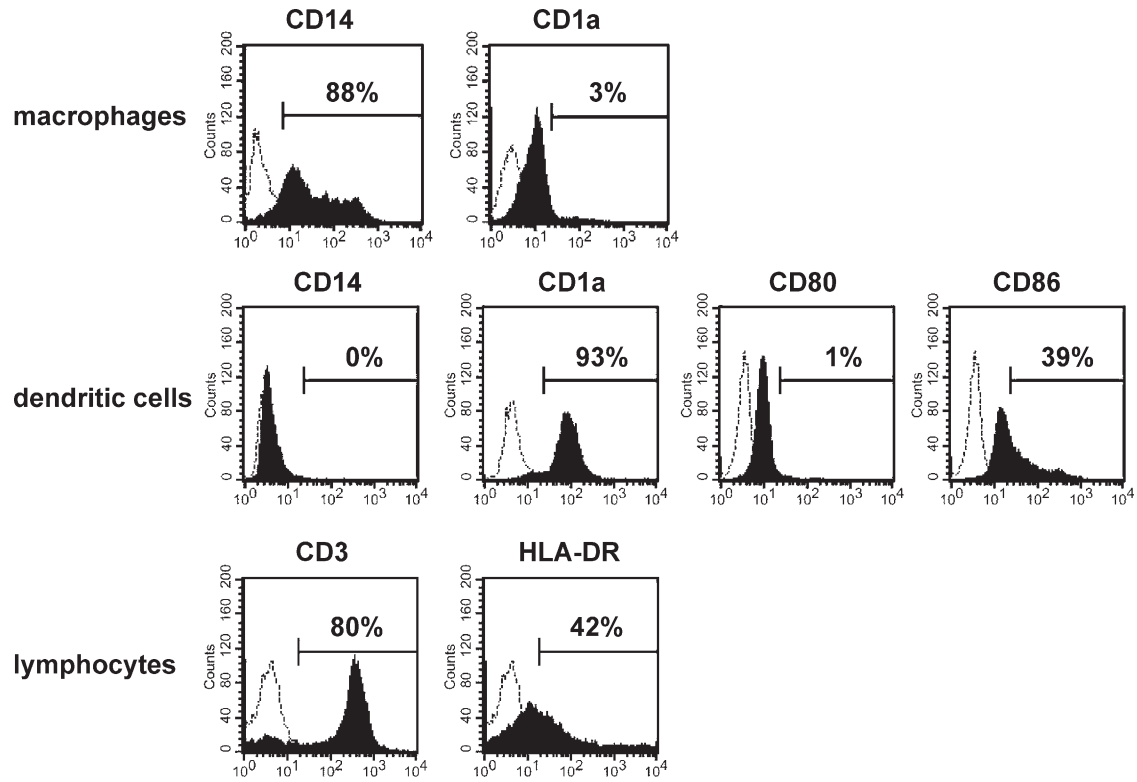


**Figure S6. Phenotypic characterization of primary macrophages, DCs, and lymphocytes before infection.** Flow cytometry analysis was performed in lymphocytes 3 d after PHA-activation and in DCs and macrophages 5–7 d after differentiation. Dotted lines represent staining with appropriate isotype controls. The experiment is representative of three independent experiments done on different blood donors.